NAVAL POSTGRADUATE SCHOOL

MONTEREY, CALIFORNIA

THESIS

LONG-RANGE FORECASTING OF ARCTIC SEA ICE

by

Megan M. Stone

June 2010

Thesis Advisor: Tom Murphree
Thesis Co-Advisor: David Meyer

Approved for public release, distribution is unlimited

THIS PAGE INTENTIONALLY LEFT BLANK

1. AGENCY USE ONLY *(Leave blank)*	**2. REPORT DATE** June 2010	**3. REPORT TYPE AND DATES COVERED** Master's Thesis	
4. TITLE AND SUBTITLE Long-Range Forecasting of Arctic Sea Ice		**5. FUNDING NUMBERS**	
6. AUTHOR(S) Megan M. Stone			
7. PERFORMING ORGANIZATION NAME(S) AND ADDRESS(ES) Naval Postgraduate School Monterey, CA 93943-5000		**8. PERFORMING ORGANIZATION REPORT NUMBER**	
9. SPONSORING /MONITORING AGENCY NAME(S) AND ADDRESS(ES) N/A		**10. SPONSORING/MONITORING AGENCY REPORT NUMBER**	

11. SUPPLEMENTARY NOTES The views expressed in this thesis are those of the author and do not reflect the official policy or position of the Department of Defense or the U.S. Government. IRB Protocol number ___N/A____.

12a. DISTRIBUTION / AVAILABILITY STATEMENT Approved for public release; distribution is unlimited	**12b. DISTRIBUTION CODE**

13. ABSTRACT (maximum 200 words)

The operational production of skillful long-range forecasts of Arctic sea ice has the potential to be very useful when integrated into the planning of Arctic operations by the U.S. Navy and other organizations. We investigated the potential for predicting October sea ice concentration (SIC) in the Beaufort Sea at lead times of one to five months. We used SIC data for 1979–2007 to statistically and dynamically analyze atmospheric and oceanic processes associated with variations of SIC in the Beaufort Sea. We also conducted correlation analyses to identify climate system variables for use as predictors of SIC. We developed linear regression models for predicting SIC based on multiple predictors. We tested these models by generating hindcasts of October SIC for 1979–2007 based on several combinations of predictors. We found two key predictors of October SIC in the Beaufort Sea at leads of one to five months—antecedent SIC in the Beaufort Sea and sea surface temperature (SST) in the Caribbean Sea in the preceding May-September period. Both of these predictors showed a consistent and statistically significant relationship with October SIC at all lead times. Both are also dynamically reasonable predictors, given the role of antecedent ice conditions and of the Arctic Oscillation and North Atlantic Oscillation in influencing basin scale SSTs. Our hindcast verification metrics show that a linear regression model based on these two predictors produces skillful forecasts of SIC at leads of one to five months. Based on these results, we issued a forecast on 01 June 2010 for SIC in the Beaufort Sea in October 2010. We also identified and conducted multi-year, linear regression hindcasts using several other predictors (e.g., low level air temperature, low level winds, and upper ocean temperature) that proved useful at various lead times. Our results indicate a significant potential for improving long range forecasts in support of Arctic operations by the U.S. Navy and other organizations.

14. SUBJECT TERMS Arctic, Sea Ice, Sea Ice Concentration, Beaufort Sea, Military Operations, Climate, Climatology, Climate Analysis, Climate Prediction, Long-range Forecast, Statistical Forecast, Meteorology, Arctic Oscillation, North Atlantic Oscillation, Caribbean Sea	**15. NUMBER OF PAGES** 117
	16. PRICE CODE

17. SECURITY CLASSIFICATION OF REPORT Unclassified	**18. SECURITY CLASSIFICATION OF THIS PAGE** Unclassified	**19. SECURITY CLASSIFICATION OF ABSTRACT** Unclassified	**20. LIMITATION OF ABSTRACT** UU

i

THIS PAGE INTENTIONALLY LEFT BLANK

LONG RANGE FORECASTING OF ARCTIC SEA ICE

Megan M. Stone
Civilian, United States Navy
B.S., Atmospheric Science, University of North Carolina at Asheville, 2008
B.S., Applied Mathematics, University of North Carolina at Asheville, 2008

Submitted in partial fulfillment of the
requirements for the degree of

MASTER OF SCIENCE IN METEOROLOGY

from the

**NAVAL POSTGRADUATE SCHOOL
June 2010**

Author: Megan M. Stone

Approved by: Tom Murphree
                       Advisor

                       David Meyer
                       Co-Advisor

                       Phillip Durkee
                       Chairman, Department of Meteorology

THIS PAGE INTENTIONALLY LEFT BLANK

ABSTRACT

The operational production of skillful long-range forecasts of Arctic sea ice has the potential to be very useful when integrated into the planning of Arctic operations by the U.S. Navy and other organizations. We investigated the potential for predicting October sea ice concentration (SIC) in the Beaufort Sea at lead times of one to five months. We used SIC data for 1979–2007 to statistically and dynamically analyze atmospheric and oceanic processes associated with variations of SIC in the Beaufort Sea. We also conducted correlation analyses to identify climate system variables for use as predictors of SIC. We developed linear regression models for predicting SIC based on multiple predictors. We tested these models by generating hindcasts of October SIC for 1979–2007 based on several combinations of predictors. We found two key predictors of October SIC in the Beaufort Sea at leads of one to five months—antecedent SIC in the Beaufort Sea and sea surface temperature (SST) in the Caribbean Sea in the preceding May-September period. Both of these predictors showed a consistent and statistically significant relationship with October SIC at all lead times. Both are also dynamically reasonable predictors, given the role of antecedent ice conditions, and of the Arctic Oscillation and North Atlantic Oscillation in influencing basin scale SSTs. Our hindcast verification metrics show that a linear regression model based on these two predictors produces skillful forecasts of SIC at leads of one to five months. Based on these results, we issued a forecast on 01 June 2010 for SIC in the Beaufort Sea in October 2010. We also identified and conducted multi-year, linear regression hindcasts using several other predictors (e.g., low level air temperature, low level winds, and upper ocean temperature) that proved useful at various lead times. Our results indicate a significant potential for improving long range forecasts in support of Arctic operations by the U.S. Navy and other organizations.

THIS PAGE INTENTIONALLY LEFT BLANK

TABLE OF CONTENTS

LIST OF FIGURES

xiii

LIST OF TABLES

LIST OF ACRONYMS AND ABBREVIATIONS

AK   Alaska

AN   above normal

AO   Arctic Oscillation

AOI   AO Index

ARCUS   Arctic Research Consortium of the United States

ARGO   Advanced Research and Global Observation

ASIV   anomalous sea ice variability

AVHRR   Advanced Very High Resolution Radiometer

BN   below normal

BonD   Battlespace on Demand

BS   Beaufort Sea

BSI   Barnett Severity Index

CBA   capabilities based assessment

CIS   Canadian Ice Service

CNMOC   Commander, Naval Meteorology Oceanography Command

CNO   Chief of Naval Operations

COADS   Comprehensive Ocean-Atmospheric Data Set

CS   Caribbean Sea

DMSP   Defense Meteorological Satellite Program

DoD   Department of Defense

ECMWF   European Centre for Medium-Range Weather Forecasts

EN   El Nino

ENLN   El Nino - La Nina

ENSO	El Nino Southern Oscillation
ERA	ECMWF reanalysis
ESRL	Earth Systems Research Laboratory
FAR	false alarm rate
FNMOC	Fleet Numerical Meteorology and Oceanography Center
GCM	general circulation model
GPH	geopotential height
HDD	heating degree days
hPa	hectoPascal
HSS	Heidke skill score
IC	Icelandic Low
IIP	International Ice Patrol
LN	La Nina
LRF	long-range forecast
m	meter
MAE	mean absolute error
mb	millibar
MEI	Multivariate ENSO Index
NAIS	North American Ice Service
NAME	Naval Postgraduate School pan-Arctic coupled ice-ocean model
NAO	North Atlantic Oscillation
NAOI	NAO Index
NASA	National Aeronautics and Space Administration
NAVO	Naval Oceanographic Office

NCAR	National Center for Atmospheric Research
NCEP	National Centers for Environmental Predication
NIC	National/Naval Ice Center
Nino3.4	SST based index of ENLN
NOAA	National Oceanic and Atmospheric Administration
NODC	National Oceanographic Data Center
NPS	Naval Postgraduate School
NSIDC	National Snow and Ice Data Center
NSR	Northern Sea Route
NW	northwest or northwest Canada
NWP	Northwest Passage
PC	percent correct
PIOMAS	Pan-Arctic Ice Ocean Modeling Assimilation System
PNA	Pacific North American
PNAI	PNA Index
POD	probability of detection
POP	Parallel Ocean Program
RMSE	root mean squared error
SEARCH	Study of Environmental Arctic Change
SIC	sea ice concentration
SIE	sea ice extent
SMMR	scanning multichannel microwave radiometer
SODA	Simple Ocean Data Assimilation
SOI	Southern Oscillation Index
SSI	spectral statistical interpolation

SSM/I	special sensor microwave / imager
SST	sea surface temperature *or* surface skin temperature
T	temperature
TAO/TRITON	Tropical Atmospheric-Ocean/Triangle Trans-Ocean Buoy Network3
TFCC	Task Force Climate Change
u	zonal wind or zonal current
v	meridional wind or meridional current
WHOI	Woods Hole Oceanographic Institute
Z	geopotential height

ACKNOWLEDGMENTS

THIS PAGE INTENTIONALLY LEFT BLANK

I.   INTRODUCTION

A.   BACKGROUND

In May 2009, the Chief of Naval Operations (CNO) formally reviewed plans for operations in the Arctic region due to recently observed climate changes in the region. This review led to the establishment of the Task Force Climate Change (TFCC). The TFCC published the United States Navy Arctic Roadmap in October 2009 (TFCC 2009). The Roadmap states that the sea ice decline in the Arctic may lead to increased resource development, research, and tourism, and could reshape the global transportation system. Reducing the uncertainty in the projections of these changes will enable the Navy to make better-informed investment and policy decisions (TFCC 2009).

The Roadmap describes a number of research, education, operational and other objectives. The accomplishment of these objectives is intended to provide Navy decision makers with a better understanding of the current and predicted Arctic environment on temporal and spatial scales that would support the planning of naval tactics, operations, and strategies (TFCC 2009). One of the major objectives of the Roadmap is to understand when significant access for Arctic shipping and other maritime activity is likely to develop. The desired effect of this objective is to develop a better understanding of the changes and projections for the Arctic environment, specifically when the sea ice will recede and to what extent the sea ice recession would allow maritime access into the Arctic that would otherwise not be possible (TFCC 2009).

Section 4.5 of the Roadmap, entitled *environmental assessment and prediction*, states that the Navy desires to understand the changes and projections for the Arctic environment, specifically when and to what extent ice will recede and allow increased maritime access to the Arctic (TFCC 2009). The Roadmap states that one of the ways the Navy will achieve this goal is by initiating a capabilities based assessment (CBA) of the Navy's Arctic observing,

mapping, and environmental prediction capabilities (TFCC 2009). The CBA will evaluate the Navy's capability and requirements to: (a) observe the physical environment in the Arctic region, to include hydrographic, atmospheric, oceanographic, and ice data; and (b) predict air-sea-ice conditions on different strategic time scales, including months to decades (TFCC 2009). As shown in Figure 1, *environmental assessment and prediction* underpins the rest of the Arctic Roadmap focus areas (Titley 2009). If the Navy does not have a full understanding of the Arctic climate system, then the other focus areas will not function to their full potential. The purpose of our study is to develop skillful long-range forecasts (LRFs) of sea ice in the Arctic. This study was designed to help meet the objectives of the Arctic Roadmap by developing and testing methods for producing skillful LRFs of Arctic sea ice. The overall goal of our study is to advance the Navy's understanding of the physical environment and help improve long-range planning of Arctic operations.
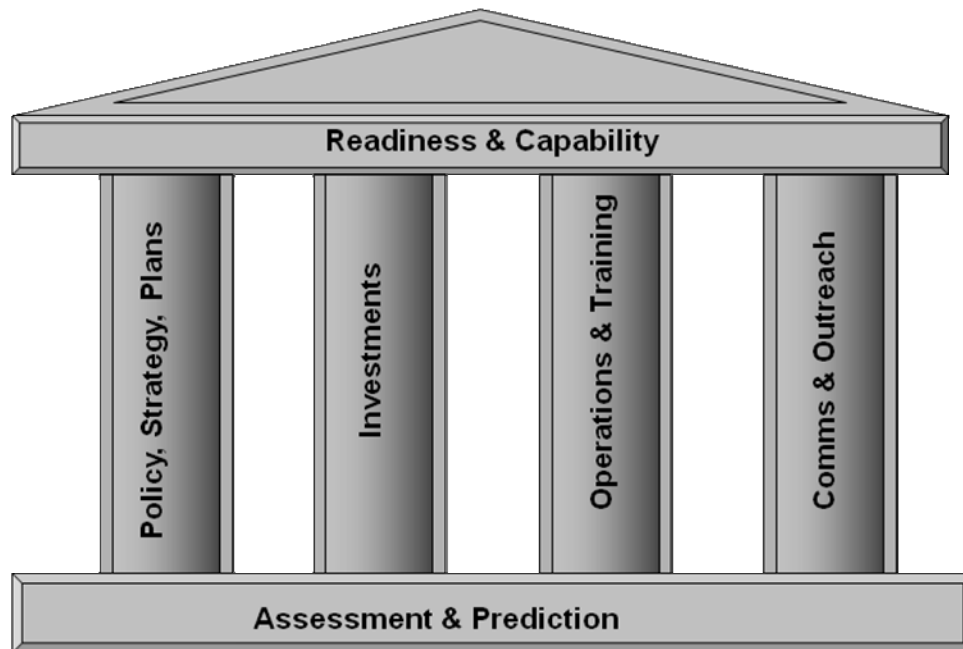
Figure 1.   Schematic diagram of the Navy's plan for dealing with climate change in the Arctic. The six focus areas are represented as pillars. Climate assessment and prediction is the foundation of the other focus areas. Our study is viewed as important for improving the navy's ability to assess and predict Arctic sea ice. Image from Titley (2009).

Climate change in the Arctic has been a widely researched topic among scientists. Figure 2 shows a time series of Arctic sea ice extent in April from 1979 to the present. Arctic sea ice in April has decreased by approximately 2.6% per decade since 1979 (NSIDC 2010a). These declines in April sea ice extent are similar to those for all the other months (not shown). Climate models suggest that the Arctic Ocean could experience ice-free summers by the middle-to-end of the 21st century (Maslowski 2007). This information is alarming and it is important for scientists to research what is causing these climatic changes in Arctic sea ice.
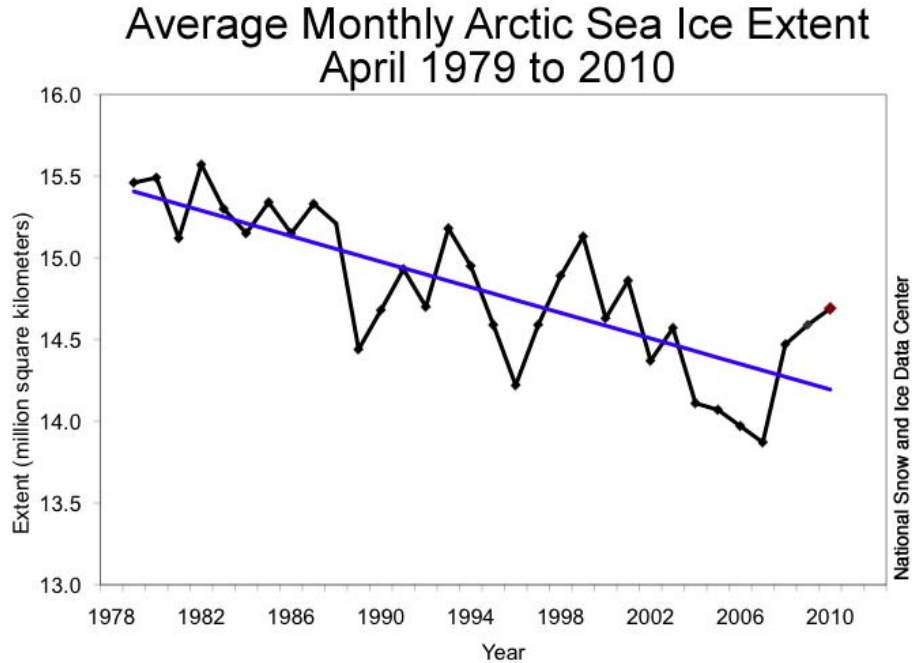
Figure 2. Arctic wide sea ice extent for April 1979–2010. Note the approximate 2.6% per decade decline since 1979. Image from NSIDC (2010a).

Understanding Arctic sea ice variation in specific regions of interest within the Arctic is critical in developing a LRF of sea ice at lead times of several months. While steps have been taken to understand what causes sea ice variation in the Arctic, operational forecasts of sea ice for specific regions within the Arctic at lead times of one month or greater are still not as reliable and operationally useful as is needed by Navy decision makers (cf. TFCC 2009). In this study, we have focused on how state of the science data sets, and analysis and forecasting methods, can be used to generate skillful LRFs of Arctic sea ice anomalies at lead times of one to five months in support of potential naval operations and navigation in the Arctic.

B. PRIOR WORK AND EXISTING ARCTIC SEA ICE PRODUCTS

1. Definitions

Sea ice concentration (SIC) is the fraction or percentage of the ocean area that is covered by ice. SIC is non-dimensional (no units). Sea ice extent (SIE) is defined as the area of the ocean that contains at least 15% SIC. The standard unit for SIE is km^2. The term *ice free* refers to the area of the ocean that contains less than 15% SIC. These definitions and those of other related terms are available at the National Snow and Ice Data Center (NSIDC) web site (NSIDC 2010c).

2. Prior Research

A number of prior studies have investigated Arctic sea ice variations and methods for predicting those variations.

Lindsay et al. (2007) showed that the SIE for the entire Arctic declined in both March (maximum sea ice extent month) and September (minimum sea ice extent month) during 1958–2005 (Figure 3). They constructed a statistical forecast model to predict Arctic-wide September SIE using four atmospheric teleconnection indices and sea ice variables extracted from the Pan-Arctic Ice-Ocean Modeling Assimilation System (PIOMAS). For information regarding PIOMAS, see Section 3.a. Their study concluded that the most viable way to predict Arctic SIE in September is to consider SIC in the early summer. Above (below) average SIC in the early summer months lead to anomalously high (low) sea ice extent in September. At longer lead times, they suggested using Arctic ocean temperatures as the primary predictor, given that ocean climate variations tend to occur on longer timescales than those in the atmosphere and the overlying sea ice.
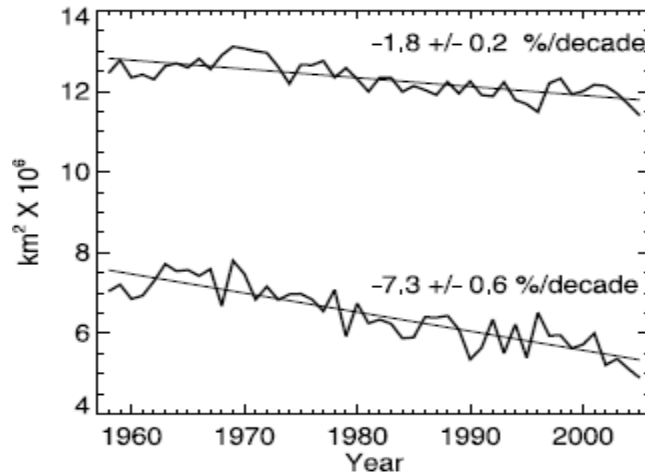
Figure 3.   Estimated Arctic wide sea ice extent for March (upper) and
September (lower) from 1958–2005. The black lines through the time series
show the linear trend for the 48-year period. See main text for information
pertaining to how the data was obtained. Image from Lindsay (2008).

Barnett (1980) showed that when SIC increased (decreased) north of
Alaska during the summer and fall seasons, a strong (weak) Siberian high and
weak (strong) Arctic high tended to occur in the preceding months. Barnett
argued that a strong (weak) Arctic high leads to anomalous easterly (westerly)
winds through the Beaufort Sea and Chukchi Seas. These anomalous winds
result in an anomalous westward (eastward) transport of ice through the Beaufort
Sea, resulting in less (more) ice and favorable (unfavorable) conditions for
navigation. Barnett developed an LRF method for predicting sea ice north of
Alaska based on the sum of 1000 hPa geopotential heights in April at two
different geographical points. In this method, if the sum of the 1000 hPa
geopotential heights is greater (less) 290 m, then sea ice is predicted to be
higher (lower) than average in the late summer and fall months in the Beaufort
Sea. Drobot (2003) showed that the Barnett LRF method showed relatively good
skill for the years 1953 through 1975, but that it did not validate well from 1975
through 2000.

Barnett (1980) led to the development of the Barnett Severity Index (BSI),
an index that monitors the severity of summer sea ice in the Beaufort Sea. The

6

BSI is a linear combination of the following: 1) the distance in nautical miles from Point Barrow northward to the ice edge on 15 September, 2) the distance from Point Barrow, AK, northward to the 4/8th ice concentration line on 15 September, 3) the number of days the entire sea route from the Bering Strait to Prudhoe Bay is ice free in a calendar year, 4) the number of days the entire sea route from Prudhoe Bay is less than or equal to 4/8th ice concentration in a calendar year, and 5) the temporal length of the navigable season, defined as the time period from the initial date the sea route is less than 4/8th ice concentration to 1 October (Drobot 2003).

Drobot (2003) investigated methods to forecast the BSI at lead times of several months using 16 different atmospheric teleconnection indices, sea ice concentration, and heating degree days (HDD) at Point Barrow as possible predictors. Drobot found that the most significant predictor of the BSI was sea ice concentration in the preceding months, specifically the multiyear ice gradient and the total ice concentration in the Beaufort Sea. HDDs were the least significant predictor.

Liu et al. (2004) found that sea ice tends to decrease (increase) in the Greenland Sea, the Barents Sea, and the Sea of Okhotsk (the Bering Sea, the southern Chukchi/Beaufort Seas, and the Northwest Passage) during a positive phase of the Arctic Oscillation (AO) due to an increase of warm (cold) air advection resulting from altered wind patterns. Liu et al. (2004) also found that: (a) the Hadley circulation in the eastern tropical Pacific (tropical Atlantic) tends to intensify (relax) during El Niño events due to the increased (decreased) pole-to-equator meridional temperature gradient; (b) the increased (decreased) Hadley circulation results in an increased (decreased) Ferrel circulation and therefore an increase of anomalous poleward (equatorward) mean meridional heat flux into the Arctic; and (c) the net result of these changes is increased (decreased)Arctic air temperature that limits (encourages) Arctic sea ice growth.

However, Comiso et al. (2008) and Deser and Teng (2008) found that the AO may have been a major factor driving Arctic sea ice variability in the past but

has not been such a strong factor in recent years . Comiso et al. (2008) showed that despite decadal scale changes in the sign and intensity of the AO and the North Atlantic Oscillation (NAO), sea ice coverage in the Arctic has continued to decline 9–10% per decade. They suggest that warming conditions in the Arctic may be overriding the connection between these two oscillations and Arctic sea ice variability. Deser and Teng (2008) found that the AO was predominately positive from 1979–1993 and that the overall Arctic SIC trends in that period were consistent with what would be expected during a positive AO based on the findings of Liu et al. (2004). However, for the more recent period of 1993–2006, Deser and Teng found that the AO was predominately negative, but the SIC trends were not consistent with what would be expected during a negative AO based on Liu et al. (2004). Deser and Teng showed that the Arctic region experienced an overall net decrease in SIC from 1993–2006, despite the decadal scale change in the phase of the AO.

Tseng (2010) extracted several atmospheric variables from the European Centre for Medium-Range Weather Forecasts Reanalysis-15 to investigate possible connections between anomalous sea ice variability (ASIV) in the Arctic and different atmospheric parameters. Sea ice data for this study was extracted from the Naval Postgraduate School (NPS) pan-Arctic coupled ice-ocean model (NAME). Atmospheric parameters tested were 2-m temperature, downward shortwave and longwave fluxes, and 10-m zonal and meridional winds and stresses. Tseng found that the atmospheric parameter having the largest influence on ASIV was anomalous surface air temperature. Their results also showed that atmospheric forcing alone does not explain all ASIV in the Arctic.

There are several studies that investigate statistical and numerical modeling of Arctic sea ice with lead times ranging from several months to several decades. Ensemble predictions of Arctic sea ice in 2008 were investigated by Zhang et al. (2008). The model used in this study was the PIOMAS model that was also used in Lindsay et al. (2007) and is also further discussed in Section 3.a (below). The predictions from the model indicated a significant reduction in

ice thickness in 2008 due to the unusually warm sea temperatures in summer 2007 as well as record low ice cover. Maslowski et al. (2007) investigated ways to improve climate modeling of sea ice in the Arctic. They argue that existing global climate predictions are erroneous due to insufficient model resolution or inadequate physics (Maslowski et al. 2007). Sea ice and ocean models are also typically configured at fairly coarse resolutions so that they can include the entire glove and have the ability to simulate the climate system within computational restraints (Maslowski et al. 2007). These are limitations that have a negative impact on modeling sea ice in the Arctic and therefore inhibit our ability to predict future changes. In their study, they investigated the use of regional high-resolution models to approach Arctic climate studies and found that sea-ice variability can be reproduced with these models as long as the atmospheric and oceanic forcings included within the model are accurate (Maslowski et al. 2007).

3.   Examples of Existing Arctic Long-Range Sea Ice Products

Several different sea ice products are presently available from both U.S. Department of Defense (DoD) organizations and non-DoD organizations. Short-range forecasts of the Arctic are limited to lead times of several days and do not show skill at longer leads. Long-range sea ice products are more useful for operational and strategic planning of operations in the Arctic. Examples of long-range products are outlined in this section.

a.   *Non-DoD Products*

The Study of Environmental Arctic Change (SEARCH) is a non-profit, civilian, multi-agency program that is part of the Arctic Research Consortium of the United States (ARCUS; ARCUS 2010). SEARCH facilitates system-level investigations of Arctic environmental change (SEARCH 2010). One of the products issued by SEARCH is an Arctic sea ice outlook focused on the summer sea ice melt season (June-September). The emphasis is on estimates of the September sea ice minimum for the Arctic as a whole and for

specific regions within the Arctic. The outlook is based on forecasts from multiple international sources (e.g., experimental forecasts from researchers). A major objective of the sea ice outlook is to summarize all critical data to provide the Arctic science community and users of Arctic science information with the best information regarding climate change in the Arctic. The sea ice outlook provides estimates of sea ice at lead times of one to three months. However, the outlook is intended mainly as a forum for sharing analyses and experimental estimates of sea ice. It is not a source of forecasts that are ready for operational use by decision makers (e.g., Navy planners) (SEARCH 2010).

The Polar Science Center at the University of Washington has developed an experimental coupled ice-ocean ensemble forecasting system called PIOMAS, used in the study by Lindsay et al. (2007). PIOMAS forecasts sea ice thickness and extent for the entire Arctic region for lead times up to three months. The developers have stated on their website that PIOMAS still contains many uncertainties, and that the purpose of making sea ice predictions is for scientific research and education only, and should not be used for operational purposes at this time.

Lindsay et al. (2010) utilized the PIOMAS model in order to develop a forecast of September 2010 sea ice conditions near Point Barrow, Alaska. They used output from the PIOMAS model as predictors in a statistical regression-based model that was used to predict sea ice conditions. Every single prediction based on the regression model yielded below-average ice conditions near Point Barrow, Alaska for September 2010. Zhang (2010) also used the PIOMAS model to develop a forecast of September 2010 SIE in the Arctic region. They forecasted that the September 2010 SIE would be approximately 4.7 million square kilometers. This is based on ensemble predictions from the PIOMAS model starting on 01 June 2010. Both of these studies for research purposes and appear in the SEARCH 2010 sea ice outlook (SEARCH 2010).

b.   DoD Products

The North American Ice Service (NAIS) is an international organization comprised of the U.S. National/Naval Ice Center (NIC), the Canadian Ice Service (CIS), and the International Ice Patrol (IIP). One of the missions of the NAIS is to meet the marine ice information needs and obligations of the United States and Canadian governments (NAIS 2010).

The NIC and CIS jointly release a 30-day sea ice forecast bulletin that is generated on the first business day following the 1st and 15th of each month during the months of July through December of each year, and covering both eastern and western North American portions of the Arctic (NIC 2010).   The bulletins are issued as a text document and describe the expected advance or retreat of ice in the Arctic region over a 30-day period. These bulletins are intended for use by decision makers at lead times of 30 days or less.

The NIC and CIS also jointly generate a summer sea ice seasonal outlook that is released in June of the same year (NIC 2010). The outlook is issued as a text document and is developed through the analysis of ice growth regimes in conjunction with wind and temperature analyses. This outlook provides decision makers with very detailed information about the normal sea ice and meteorological regimes for the eastern and western North American portions of the Arctic and Hudson Bay, recent observations of sea ice for these regions, and a brief text outlook for the timing of sea ice break-up and freeze-up conditions based on observed and expected anomalies in air temperature and wind patterns. This outlook provides useful information on the recent and present state of sea ice in the North American region but limited textual information on upcoming sea ice conditions.

The Climatology Division at the Fleet Numerical Meteorology and Oceanography Center (FNMOC) is able to provide plots of long term mean (LTM) SIC for areas and periods of interest to customers. Such LTM products may be useful in environments that do not experience much intraseasonal to decadal

variation, since the LTM does not account for climate variations (e.g., variations such as the AO and NAO, trends such as long term declines (Figure 2)) (Murphree 2008a). If a Navy decision maker is in need of a sea ice forecast in the Arctic, FNMOC generates an image using sea ice data from the one-degree resolution Reynolds sea surface temperature (SST) reanalysis data set (Reynolds et al. 2002) displaying the LTM SIC for the customer's region and period of interest. Figure 4 shows an example of the LTM SIC for the Beaufort and Chukchi Sea regions in October as produced by FNMOC.
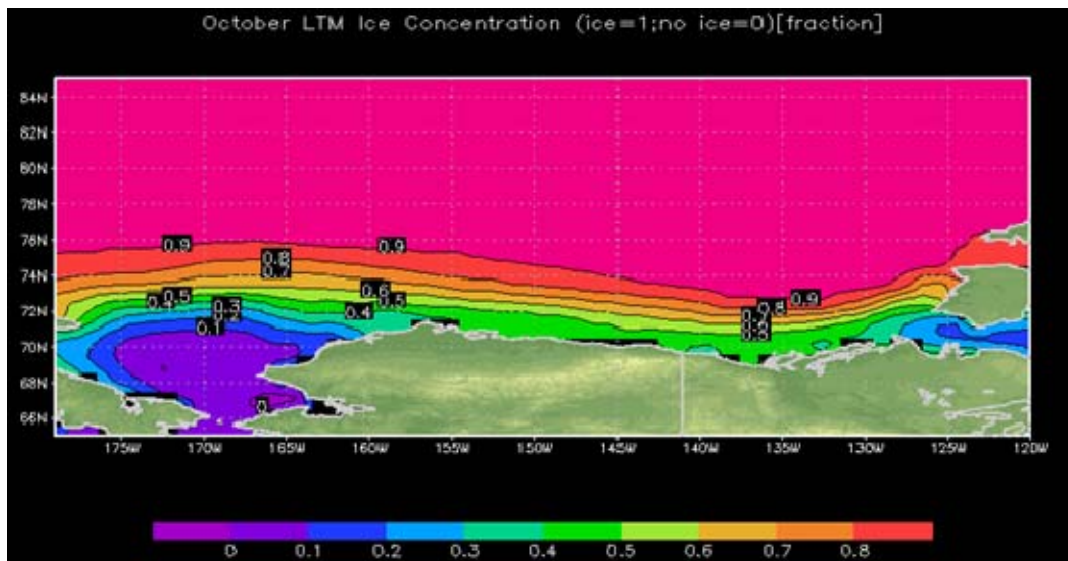
Figure 4.   Example of a LTM SIC product generated in May 2010 by FNMOC. This example shows LTM October SIC in the region of the Chukchi and Beaufort seas. The basic data for this product is SIC data from the Reynolds SST reanalysis (Reynolds et al. 2002). LTM depictions of SIC do not allow variations and trends of SIC to be displayed. Such variations and trends are important for state of the science long range climate support of naval operations in the Arctic.

Deser and Teng (2008), Comiso et al. (2008), Lindsay (2008), and others have shown that the Arctic has experienced, and continues to experience, a significant long term net decline in sea ice per decade. Barnett (1980), Drobot (2003), Liu et al. (2004), and Figure 2 clearly indicate that Arctic sea ice

12

experiences a large amount of interannual variation due to regional and global scale climate variations. Thus, products based exclusively on LTMs are not viable representations of sea ice conditions in support of naval operations. LTM products involve extensive averaging that obscures climate variations.

Our study focuses on explicitly accounting for climate variations in developing and testing methods for generating explicit, state-of-the-science LRFs of Arctic sea ice that directly support the planning of DoD operations.

4.   Improving Climatology Support Methods

The optimal climatological support process for DoD would employ: state-of-the-science: (a) data sets, such as long term, high resolution resolution reanalyses of the atmosphere, ocean, land, and ice (e.g., Kalnay et al. 1996; Kistler et al. 2001; Saha et al. 2010); and (b) methods, such as statistical and dynamical prediction methods (e.g., Wilks 2006; van den Dool 2007). These data sets and methods would be used to analyze and forecast the climate system in direct support of DoD operations. A number of prior studies have been completed at the Naval Postgraduate School (NPS) that demonstrate how improved climatology methods can be used to make significant improvements to Navy climatology support. Moss (2007), Turek (2008), Twigg (2008), Mundhenk (2009), Ramsaur (2009), and Heidt (2009), have all shown the importance of using advanced climate analysis and long-range forecasting methods to increase awareness at long lead times of the potential impacts of climate impacts on military operations.

Figure 5 shows an example of an eight step method to be followed to provide advanced climate support (Mundhenk 2009). Once the customer submits a request for climatology support, the first step is to gather the state-of-the-science, advanced data sets to be used to generate a forecast for the area and time period of interest. Step two is to analyze the climate system using advanced methods from the data sets chosen in step one. Step three is to develop a forecast method based on the climate system analysis. Step four is to

test the forecast method from step 3 by making multi-decadal hindcasts. Step five is to verify the hindcasts. If the hindcasts verify well, then step six is to develop a forecast, and step seven is to implement the generated forecast into a climate support package, including with decision support information and recommendations, that is given to the customer. The final step is to assess the support provided by: (a) verifying the forecast given to the customer and (b) analyzing how the forecast impacted the customer's mission. Based on these assessment steps, decisions can be made about how to improve the overall climate support process. In practice, many customer requests can be anticipated, so that many of these steps (e.g., steps 1–4) could be partially or fully completed in advance of receiving customer requests. For example, Navy customer requests for SIC forecasts could be anticipated for many locations, periods, and types of naval operations.
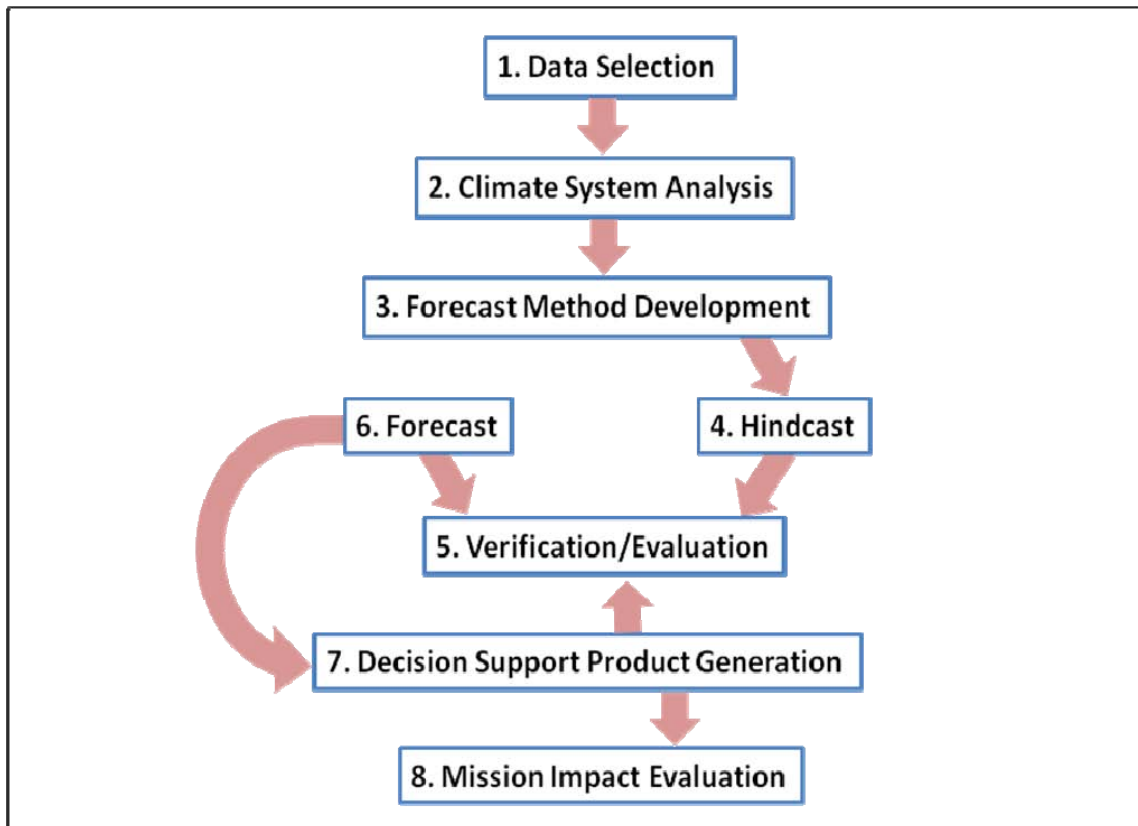
Figure 5.   Eight steps in providing advanced climate support. Image adapted from Mundhenk (2009).

C.   ACHIEVING THE ARCTIC ADVANTAGE

Predicting Arctic SIC at lead times of one to five months is a very difficult task that will require on-going and new research efforts. Not only does Arctic sea ice undergo large variations from year to year, but sea ice has been experiencing an overall declining trend (e.g., Figure 2). It is important for the Navy to understand sea ice variations and trends by taking into account the conditions in the atmosphere, ocean, and land that create them. Thus, the Navy should be researching, testing, and producing products and concepts of operations that can give Navy decision makers the best advantage for planning for planning operations in the Arctic.

The Battlespace on Demand (BonD) concept was developed by the Commander, Naval Meteorology and Oceanography Command (CNMOC) to describe the CNMOC concept of operations for providing information on the battlespace environment to warfighters (Murphree 2008a). As shown in Figure 6, the BonD concept has four tiers. Tier zero focuses on environmental observations from a variety of sources (e.g., in situ and remote sensing sources). Tier one focuses on environmental analyses and predictions based on the data from tier zero. Tier two focuses on predicting how the performance of military equipment will be affected by the conditions predicted in tier one. Tier three focuses on predicting for decision makers how to best exploit the environmental and performance conditions predicted in tiers one and two.
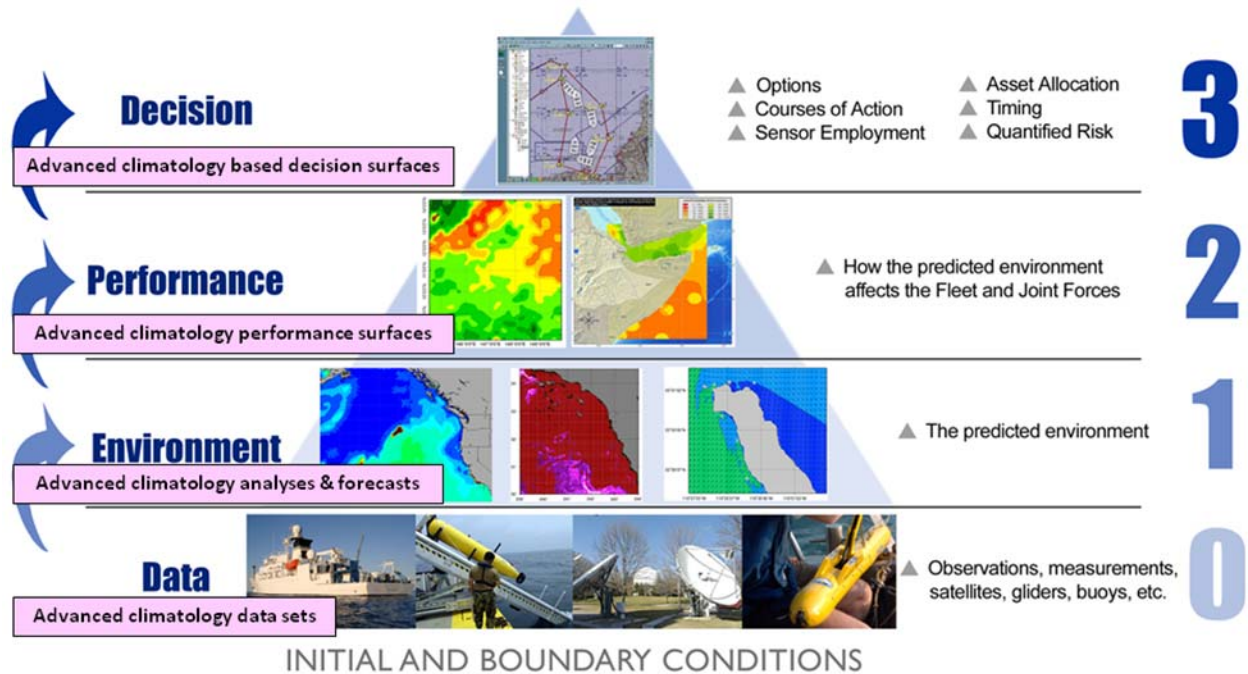
Figure 6. Schematic illustration of the Battlespace on Demand (BonD) concept of operations as developed by CNMOC for the Navy meteorology and oceanography (METOC) community. Pink boxes represent the integration of climate science based long range support within each of the four BonD tiers. Figure adapted from Murphree 2008a.

The BonD con0cept was developed to describe the concept of operations for providing environmental support for warfighters at short lead times (e.g., lead times of 0 to 72 hours). But the BonD concept also applies to long-range environmental support as well. The pink text boxes in Figure 6 describe how advanced climate science can be integrated into each tier of the BonD concept. In this study, we have used advanced climate data sets and methods to create and test methods for generating LRFs of Arctic sea ice. These LRFs are intended to be the basis for long-range environmental support at tiers two and three.

D.   SCOPE OF RESEARCH

1.   Research Questions

In our study, we researched, tested, and explored the potential for using advanced climatology data sets and methods to produce LRFs of sea ice in the Arctic in support of warfighters and other decision makers, as they plan and conduct operations in the Arctic region. This study focused mainly on answering the following research questions:

1) What atmospheric and oceanic variables are the most viable predictors of sea ice anomalies in regions of interest within the Arctic?

2) Can advanced climate data sets and methods be used to forecast sea ice anomalies in the Arctic to provide warfighters and other decision makers with an improved understanding of the environment as they plan to operate in the Arctic?

3) What are the best methods of assessing the skill and operational value of LRFs of sea ice anomalies in the Arctic?

2.   Thesis Organization

To answer these research questions, we followed a methodical approach of conducting climate analyses and creating and testing LRF methods for producing long-rage forecasts of Arctic sea ice within areas of interest.

Chapter II provides: (a) a summary of the data sets that we used in this study; (b) a description of the area and period of interest and the reasons for choosing them; (c) the methods and tools used to analyze, develop, and test LRFs of sea ice in the area and period or interest. Chapter III provides: (a) an overview of the seasonal variation of SIC within our area and period of interest; (b) a summary of the results of our LRF development and testing; and (c) a forecast issued on 01 June 2010 of SIC in the Beaufort Sea during October 2010. Chapter IV summarizes our results and provides suggestions for further research.

THIS PAGE INTENTIONALLY LEFT BLANK

II. DATA AND METHODS

A. DATA SETS

1. Sea Ice Concentrations from Nimbus-7 SMMR and DMSP SSM/I Passive Microwave Data

The sea ice data set for our study consisted of monthly mean SIC data based on satellite passive-microwave observations of the Arctic for the period October 1978—December 1979 (NSIDC 2010b). In situ, observations of sea ice are too limited spatially and temporally to be useful for long term studies of sea ice (cf. Comiso et al. 2008). We obtained the sea ice data from the National Snow and Ice Data Center (NSIDC). This data has been extensively used for Arctic sea ice research in the past. (e.g., Deser and Teng 2008). The data set is generated from brightness temperature derived from Nimbus-7 Scanning Multichannel Microwave Radiometer (SMMR) and Defense Meteorological Satellite Program (DMSP) –F8, -F11, and -F13 Special Sensor Microwave / Imager (SSM/I) radiances (NSIDC 2010b). Table 1 gives an overview of the temporal coverage used by each sensor. The spatial resolution is 25 km and the spatial coverage includes both polar regions. We were only interested in the northern hemisphere polar region data for this study. Figure 7 shows the polar stereographic projection and grid spatial coverage map for the northern hemisphere polar region used in this study.

Platform and Instrument	Time Period
Nimbus-7 SMMR	26 October 1978 - 20 August 1987
DMSP –F8 SSM/I	9 July 1987 - 31 December 1991
DMSP –F11 SSM/I	3 December 1991 - 30 September 1995
DMSP –F13 SSM/I	3 May 1995 - 31 December 2007
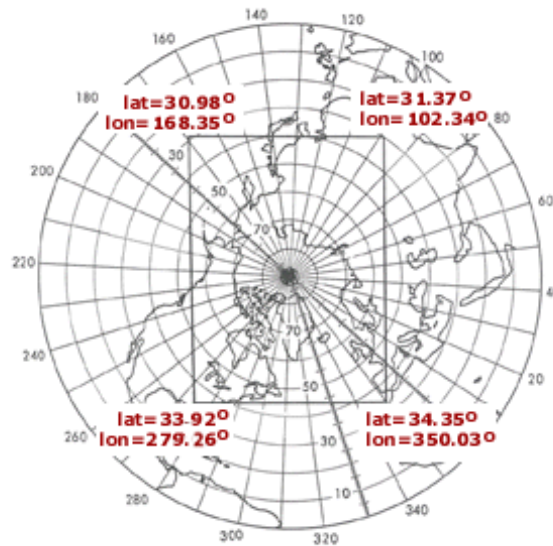
Figure 7.   The region of the Arctic covered by the SIC data set used in this study is outlined by the rectangular box centered near the North Pole. The latitudes and longitudes of the corners of the box are shown in red text. Figure from NSIDC 2010b.

The temporal coverage of the SIC data set is from October 1978 to December 2007 (NSIDC 2010b). For our study, we used the monthly mean SIC from January 1979 to December 2007, containing data for 348 months (29 years). The SMMR instrument scanner operated on every other day due to power limitations. As a result, the SMMR data was collected every other day, so a typical month contained at least 14 days of coverage. SSM/I data was

collected every day. The data set we used represents a merger of data from both sensors. The merged data set provides a uniform time series of SIC spanning the coverage of several passive microwave sensors. To accomplish this merger, sea ice algorithm coefficients were adjusted to account for differences in sea ice extent and area estimates when using the SMMR and SSM/I sensors (NSIDC 2010b). The merger of the data from the two sensors was accomplished using the National Aeronautics and Space Administration (NASA) algorithm developed by the Ocean and Ice Branch, Laboratory for Hydrospheric Processes at the NASA Goddard Space Flight Center (NSIDC 2010b).

Both the SMMR and SSM/I data sets have gaps in their coverage near the north pole due to inclinations in their orbits. These gaps differ for the two sensors due to orbital differences. The SMMR polar gap has a radius of approximately 611 km centered on the North Pole, so that the gap extends poleward from 84.5° N. The SSM/I instrument polar gap has a radius of approximately 311 km, so that the gaps extends poleward from 87.2° N (NSIDC 2010b). For our study, we removed SSM/I data from 84.5° to 87.2° to make the polar gap the same size as the SMMR data, so that the data set has a consistent polar gap from beginning to end. Our primary interest was in long-range forecasting of sea ice in areas where SIC varies by large amounts. At and near the north pole, these variations tend to be small compared to other areas of the Arctic. Thus, the polar gaps were not a significant problem for our study.

In December 2007, the processing of this SIC data set was briefly postponed due to the loss of the DMSP -F13 satellite. NSIDC is currently working with Remote Sensing Systems (RSS) to acquire the SIC data from the DMSP -F17 satellite to calibrate with the October 1978—December 2007 SIC data set. They estimated that the data will be processed and available by June 2010. By the time our project concluded in June 2010, NSIDC had not completed the calibration. Thus, the last date for the SIC data we used in this study was December 2007.

21

2. NCEP / NCAR Atmospheric Reanalysis

Our atmospheric data came from the National Centers for Environmental Prediction (NCEP) / National Center for Atmospheric Research (NCAR) reanalysis (R1) data set (Kalnay et al. 1996; Kistler et al. 2001). The R1 data set is the result of a global retrospective analysis (i.e., a reanalysis) of climate system observations from January 1948 to the present. The reanalysis uses data assimilation, spectral statistical interpolation (SSI), and dynamical analysis processes that are the same for all times. The dynamical analysis uses a T62/28-level global spectral model. In situ and remote observational data used in the R1 process include: global rawinsonde data, Comprehensive Ocean-Atmospheric Data Set (COADS) surface marine data, aircraft observations, surface land synoptic data, satellite sounder data, SSM/I surface wind speeds, and satellite cloud drift winds (Kalnay et al. 1996). All data in the NCEP/NCAR Reanalysis is run through a monitoring system to perform quality control checks. The R1 data has a spatial resolution of 2.5° at standard tropospheric and stratospheric levels, and has a temporal resolution of six hours (Kalnay et al. 1996).

We chose this data set for a number of reasons. In particular, the R1 data set has the capacity to capture low frequency climate variations, it is very accessible to the scientific community, and it has been used extensively in past Arctic research. In addition, the NOAA Earth Systems Research Laboratory (ESRL) website provides advanced plotting and data analysis tools for R1 data that aided us in the process of selecting possible predictors of SIC in the Arctic. The main R1 variables that we used in the study were 850 hPa geopotential heights (m), surface skin temperature (°C), surface vector wind (m/s), and surface air temperature (°C). Section C1 discusses how we used the ESRL mapping tools to test these variables to aid in the process of selecting potential predictors of SIC.

3. Simple Ocean Data Assimilation (SODA) Oceanic Reanalysis

The Simple Ocean Data Assimilation (SODA) reanalysis data set is a global reanalysis of the ocean covering January 1958 to December 2008 (Carton et al. 2000; Carton and Geise 2008). Like the R1 data set, the SODA data set was developed by assimilating and dynamically analyzing ocean in situ and remote ocean observations using a fixed set of data assimilation and dynamical ocean model analysis processes. The in situ observations incorporated into the SODA reanalysis include: hydrographic profile data, ocean station data, moored temperature and salinity observations, and surface temperature. Most of this data set was acquired from the World Ocean Database 2001. Additional observational data included data from the National Oceanographic Data Center (NODC), NOAA temperature archive, Tropical Atmospheric-Ocean / Triangle Trans-Ocean Buoy Network (TAO/TRITON) mooring thermistor array, Advanced Research and Global Observation (ARGO) drifter data from Woods Hole Oceanographic Institute (WHOI), and bucket temperatures from the COADS were also used. Remote sensing data incorporated into the SODA reanalysis included the NOAA/ NASA Advanced Very High Resolution Radiometer (AVHRR) operational SST, Quikscat winds, and satellite altimetry data. In order to reduce error associated with surface skin temperature effects, only nighttime retrievals were used.

The SODA reanalysis uses a dynamical analysis process based on a numerical ocean general circulation model (GCM) that is based on Parallel Ocean Program (POP) numerics. Atmospheric forcing fields for the ocean model include daily surface wind stresses derived from the European Reanalysis (ERA)-40 reanalysis, and surface freshwater fluxes from the Global Precipitation Climatology Project.

For our study, we used SODA reanalysis data from version 2.0.2 for years 1979–2001 and version 2.0.4 for years 2000–2007. This gave us an ocean reanalysis data period that matched the 1979–2007 period of the satellite passive-microwave SIC data set from NSIDC. SODA has a spatial resolution of

approximately 0.25 degrees, a temporal resolution of five days, and a spatial coverage of 72.25°S—89.25°N and 0°-360°E. For this study, we used monthly mean fields and the full global domain, but with a focus on the Arctic. We also used the same polar stereographic projection used for the SIC data set from NSIDC shown in Figure 7. The main SODA variables we used in this study were ocean temperature (°C), zonal ocean velocity (m/s), and meridional ocean velocity (m/s).

SODA provides data at 40 vertical levels ranging from 5 m to 5374 m. Table 2 overviews the vertical spatial coverage used for each variable in this study. Only the highest depth was used to represent ocean temperature close to the sea surface (e.g., at or just below the base of the sea ice). However, we investigated the relationships between the temperatures at the uppermost three levels and found them to be very well correlated. To represent upper ocean currents, we averaged the ocean velocity variables from the 5 m to 57 m. This averaging was done mainly to obtain an integrated representation of the net currents and advections likely to affect sea ice.

Table 2.   Vertical extents used in this study for the SODA oceanic variables used in this study..

Oceanic Variable	Vertical Extent
upper ocean temperature (°C)	5 m depth only
zonal ocean velocity (m/s)	5-57 m
meridional ocean velocity (m/s)	5-57 m

We checked the validity of the SODA data set by visually comparing LTM ocean currents in the Arctic region as depicted by the SODA data set and by Tomczak and Gidfrey (1994). We found that the two depictions were very similar and concluded that SODA provides a reasonable representation of at least LTM Arctic ocean circulations. Prior studies have found that SODA also provides realistic depictions of ocean climate variations in the tropics, midlatitudes, and

subpolar regions (e.g., Carton et al. 2000; Carton and Geise 2008; Heidt 2009). For more detailed information on the SODA data set and its applications in ocean climate analysis and long range forecasting, refer to Carton et al. (2000), Carton and Geise (2008), and Heidt (2009).

4.   Climate Variation Indices

We investigated the relationships between Arctic SIC and four different global scale atmospheric variations: (a) El Niño - La Niña (ENLN), Arctic Oscillation (AO), North Atlantic Oscillation (NAO), and the Pacific North American (PNA) teleconnection pattern. To represent ENLN, we used three indices: the Southern Oscillation Index (SOI), Nino 3.4 index (Nino3.4), and Multivariate El Niño – Southern Osciallation Index (MEI). To represent the AO, NAO, and PNA, we used the AO index (AOI), NAO index (NAOI), and PNA index (PNAI). Further information on these variations and indices is available from Earth Systems Research Laboratory (ESRL 2010), which was also the source of the time series data for these indices that we used in this study.

B.   FOCUS REGION, FOCUS PERIOD, AND PREDICTAND SELECTION

1.   Focus Region

We conducted analyses for the entire Arctic but chose as our focus region the Beaufort Sea. Figure 8 shows the Beaufort Sea region that we defined for our focused analyses and forecasts. This region is extends from approximately 70°N to 72°N and from 148°W to 128°W.

Figure 8.   Beaufort Sea study region used in this study (white box). This area
lies between approximately 70° - 72°N and 148° - 128°W. Background image
from Google Earth, accessed March 2010.

Our reasons for choosing this focus region were both operational and
scientific. There are two major sea navigation routes in the Arctic—the
Northwest Passage (NWP) and the Northern Sea Route (NSR), as illustrated in
Figure 9. The NWP extends along the northern coast of North America, and the
NSR is extends along the Russian Arctic coast. Both routes connect the Atlantic
and Pacific Oceans and can potentially allow ships to transit through the Arctic
between the Atlantic and Pacific, if ice conditions are favorable. Our Beaufort
Sea focus region lies along he NWP, is close to the U.S. and allied territory
(Alaska and Canada), overlaps partially with the U.S. exclusive economic zone,
and contains areas of interest for resource exploration and development (e.g., oil
and gas operations).
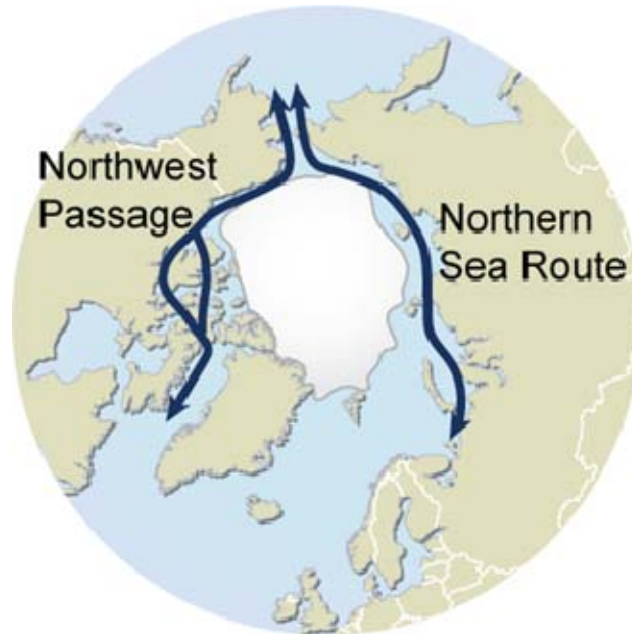
Figure 9.   The two major Arctic sea routes—the Northwest Passage (NWP) and Northern Sea Route (NSR). Image from UNEP/GRID-Arendal Maps and Graphics Library [accessed online at http://maps.grida.no/go/graphic/arctic-sea-routes-northern-sea-route-and-northwest-passage] May 2010.

SIC in the Beaufort Sea undergoes relatively large climate variations (e.g., long term declines, interannual variations). Figure 10 shows the monthly rate of SIC change during August 1987 – December 2007. The green-blue (orange-red) shading indicates a negative (positive) rate of change and a net decrease (increase) in SIC during the period. Note that large (small) areas of the Arctic experienced long term decreases (increases) in SIC. The total percent change during the period can be calculated using the total number of months during the period (245 months). For example, an area shaded in medium blue indicates a rate of change per month of -10×10^{-4}, which corresponds to a 24.5 percent total decline in SIC during the approximately 20 year period of the analysis shown in Figure 10. The Beaufort Sea is a region with relatively large long term declines. These decadal scale declines in SIC make climate analyses and long-range forecasts for this region especially important, both operationally and scientifically.

27
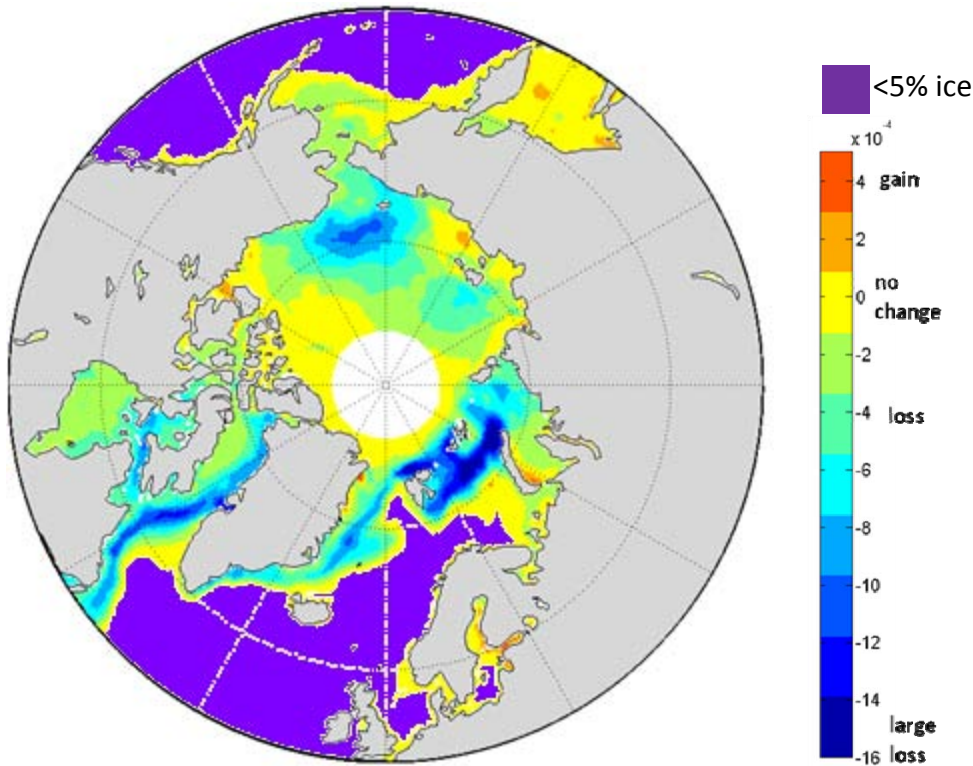
Figure 10. Rate of change of Arctic SIC per month (fractional change per month) during August 1987–December 2007. Green and blue (orange and red) indicate long term decreases (increases) in SIC. Yellow indicates no change or no ice. Purple indicates areas in which SIC was less than 5% for every month during August 1987–December 2007. The circular area near the North Pole shown in white indicates an area of no SIC data (see Chapter II, Section A.1). Note that long term decreases have been much larger in some areas than others, and that long term increases have occurred only in relatively small areas.

Figure 11 shows the standard deviation of SIC in the Arctic based on SIC data for January 1979 - December 2007. The Beaufort Sea is a region with relatively high annual standard deviation of SIC (0.15 to 0.4). This evidence of variability, like that shown in Figure 10, indicates that climate analyses and LRFs for the Beaufort Sea are especially important. Skillful LRFs of SIC for a basin that undergoes large SIC variations will tend to be more valuable than those for basins with little or no SIC variation. For low variability areas, LTMs will tend to provide relatively good indications of future conditions.

Sea Ice Concentration Standard Deviation
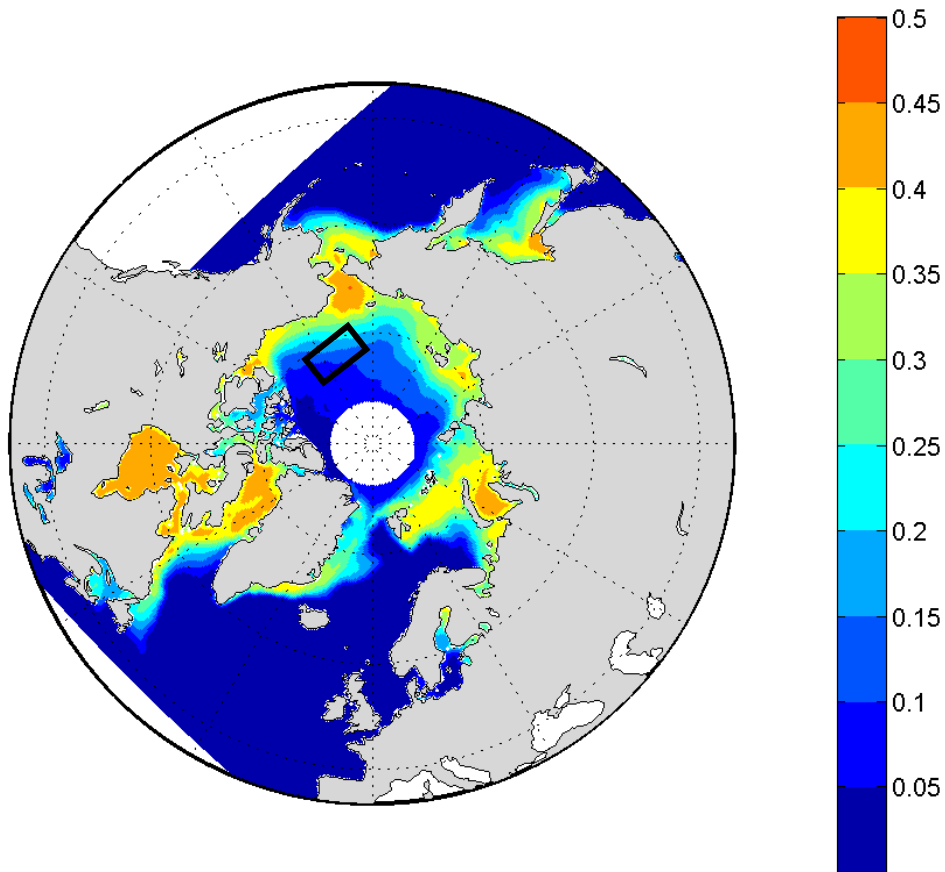
Figure 11.   Standard deviation of Arctic sea ice based on SIC data from January 1979 - December 2007. The Beaufort Sea region (outlined by black box) has a SIC standard deviation of approximately 0.15 to 0.4.

2.   Focus Period

We conducted analyses for the entire period of our SIC data set, January 1979 to December 2007, but we chose to focus on the summer August-October period of minimum SIC—and on October in particular. Figure 12 shows a time series of the LTM seasonal cycle of SIC the Beaufort Sea. August-October is the period with the lowest average SIC in the Beaufort Sea, and when the atmosphere and ocean are most likely to be switching from conditions which are favorable for melting to conditions which are favorable for freezing. Thus, this is an especially important period from an operational (e.g., navigation) perspective. All three of these months display a high variation of SIC in the Beaufort Sea

(Figure 13). September has been and is the focus period for many sea ice prediction efforts, since that it is when Arctic wide SIE is at its minimum. We chose to focus our LRF efforts on October because October tends to have: (a) low SIC values; (b) large increases in SIC; and (c) high variability in the Arctic and globally as the northern hemisphere transitions from summer to winter (cf. Turek 2008; Ramsaur 2009; Heidt 2009). These features of October make it an especially important and challenging month for which to develop climate analyses and LRFs of SIC.
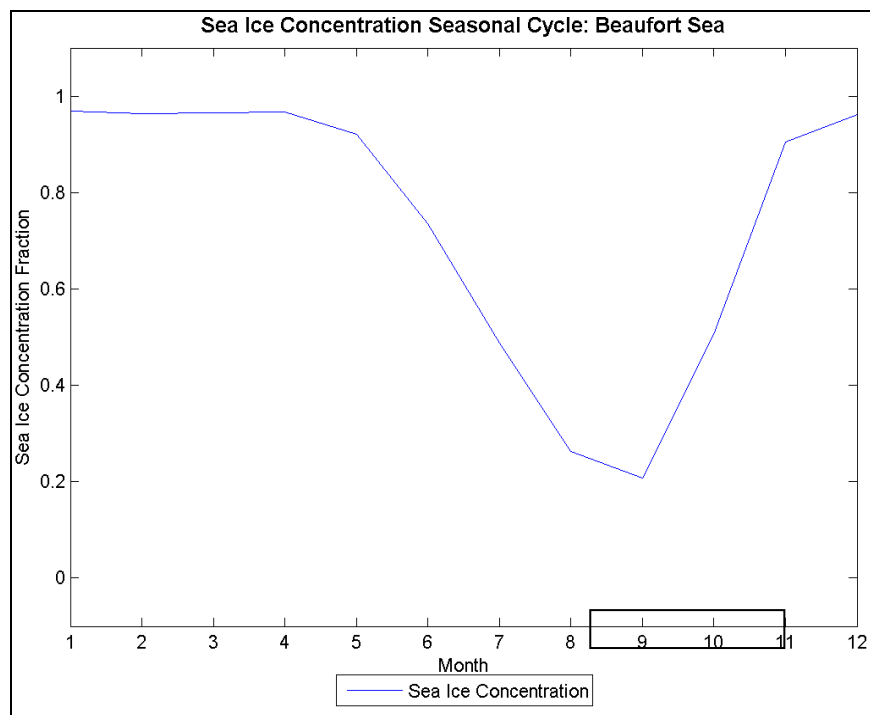
Figure 12. LTM seasonal cycle of SIC in the Beaufort Sea based on data from January 1979—December 2007. SIC is at a minimum in August—October as the Beaufort Sea transitions from conditions favorable for melting to conditions favorable for freezing.
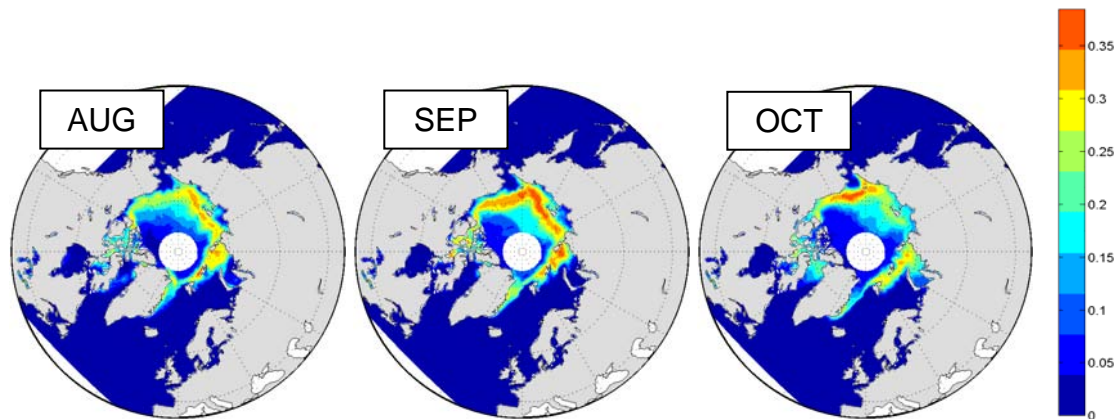
Figure 13. Average monthly SIC standard deviation in August, September, and October based on data from January 1979–December 2007. The Beaufort Sea experiences the most variability in SIC during these months.

3.   Predictand Selection

Based on our choice of focus region and focus period, we selected as our predictand (i.e., our forecast target) SIC averaged over: (a) our Beaufort Sea area; and (b) October. This is the predictand for which we developed and tested our long-range forecasting methods.

C.   ANALYSIS AND FORECASTING METHODS

1.   Composite Analyses, Correlations, and Teleconnections

We constructed the time series for our predictand—that is, a time series of SIC in the Beaufort Sea for Oct 1979-2007. From this time series, we identified the five years with the highest and lowest SIC in October. We then developed composites of global and regional conditions by averaging the conditions during the five high years and five low years. We used these composites to assess the patterns and processes during extreme SIC years. In particular, we used the extreme event composites to identify potential predictors of, and the dynamical processes that influence, Oct SIC in the Beaufort Sea. We focused on composites based on just the high five and low five periods because composites based on more than five events tend to include weaker events and tend to obscure important climate patterns, processes, and mechanisms of interest.

31

Our primary focus was on composites of anomalous conditions during and prior to the five high and low SIC periods. These anomalies were especially useful in: (a) analyzing the patterns and processes that may have created the anomalously high and low SIC events; and (b) identifying potential predictors of SIC. All the anomalies in our study were calculated using a base period of 1968-1996 to be consistent with the LTM base period used by the ESRL online data access, analysis, and plotting tools (ESRL 2010).

We correlated our predictand time series with a wide range of climate system variables (e.g., SST, air temperature, geopotential heights, low level winds, climate variation indices) to identify potential predictors of our predictand. We identified as the variables with the most potential as predictors those that had strong and significant correlations with the predictand when the variable led the predictand by zero to five months.

We also used the composites and correlation analyses to identify potential teleconnections and dynamical processes that affect the predictand. A teleconnection is defined as a statistical and/or dynamical linkage between remote climate system variables (e.g., atmospheric pressure in the North Atlantic and SIC in the Beaufort Sea).

2.   Potential Predictor Selection

We used the results of our composite anomaly, correlation, and teleconnection analyses to identify climate system variables for consideration as potential predictors of our SIC predictand. We considered a variable a potential predictor if it met at least one of the following criteria:

a. was identifiable in the composite analyses of the extreme high or low years of SIC. If the variable displayed anomalous patterns in the composite analyses, it was considered identifiable.

b. had a significant correlation with our predictand (October SIC in the Beaufort Sea) at leads of zero to five months. A correlation was

considered significant at the 95% level if the magnitude of the coefficient was the greater than 0.363, based on the standard normal distribution of a two tailed test (Wilks 2006).

c. was consistent with the findings in prior studies of long range forecasting of sea ice conditions in the Arctic.

After choosing the potential predictors, we compared their time series with that of the predictand at all lead times. This allowed us to: (a) visually check the predictor-predictand correlations; (b) identify intraseasonal to decadal variations in the relationships between the predictor and predictand; (c) identify periods and lead times for which the correlations were relatively strong and weak; and (d) identify case studies for additional statistical and dynamical analyses, and hindcast testing.

3.   Linear Regression

A simple linear regression model describes the relationship between a predictor variable and a predictand variable. We ran a linear regression between each selected predictor variable and our predictand (October SIC in the Beaufort Sea), with the predictor leading by one to five months. To measure the fit of each regression, we calculated the correlation coefficient (R), the coefficient of determination (R^2), and the p-value. For each lead time, we ranked the variables by their R^2 value. We considered a variable a potential predictor if it was highly ranked by its R^2 at each lead time and exhibited a low p-value. Our goal was to select an optimal combination of predictors from which to build a multivariate linear regression model to use in forecasting our predictand at leads of one to five months. We created different predictor combination options based on high R^2 values and low p-values. For more information on linear regressions, refer to Wilks (2006) or any other college-level statistics textbook.

4. Hindcasting and Forecasting

Using the multivariate linear regression equations generated from optimal combinations of predictors, we generated a hindcast of October SIC in the Beaufort Sea for each year and at each lead time. To do this, we generated a regression equation for each year using predictor and predictand data for all years 1979–2007, except the year for which the hindcast was being generated. Each resulting regression equation was then used to hindcast the predictand for the year for which the data had been removed. For example, for a one month lead hindcast for October 1979, we removed the October SIC value from 1979, as well as the corresponding predictor values for September 1979. We then performed a regression between the remaining 28 October SIC values and the remaining 28 values of each predictor in September to yield a regression equation. Then we plugged the September 1979 predictor values into the regression equation to hindcast the SIC for October 1979. We performed this method for all 29 October SIC values and for lead times of one to five months. This process is referred to as the *leave-one-out* cross validation method for developing and testing a regression based forecasting method (Wilks 2006).

This process generated a time series of 29 hindcasted values of October SIC in the Beaufort Sea for each lead time and for each combination of predictors. We compared these time series to the time series of actual October SIC in the Beaufort Sea to evaluate the performance of each model at each lead time, and to identify specific years for further investigation.

5. Verification

a. Scalar Accuracy Metrics

We assessed the hindcasts using two scalar measures of forecast accuracy: (a) mean absolute error (MAE); and (b) root mean-squared error (RMSE) (Wilks 2006). TMAE and RMSE are, except that RMSE involves squaring the errors rather than using the absolute value. For both MAE and RMSE, a value of zero indicates the forecasts were perfect, meaning that each

hindcasted average October SIC value was equal to the actual average October SIC value. Both the MAE and the RMSE can be interpreted as the magnitude of the typical forecast error.

b. Contingency Table Metrics

In this study, we used 2x2 contingency tables (Wilks 2006) to summarize and verify the results of each hindcast of October SIC in the Beaufort Sea. To apply this method, we grouped each of the 29 years of actual average October SIC values, and each of the 29 years of hindcasted October SIC values, into above normal (AN) or below normal (BN) categories. The average of the 29 actual October SIC values was 0.55061. Thus, if the SIC value (actual or forecasted) was greater than (less than or equal to) 0.55061, then the SIC was considered above (below) normal for that year. Table 3 shows an example of the contingency table into which we entered information on the number of:

(a) hindcasted AN years that matched with actual AN years (cell A in the table);
(b) hindcasted AN years that matched with actual BN years (cell B in the table);
(c) hindcasted BN years that matched with actual AN years (cell C in the table);
(b) hindcasted BN years that matched with actual BN years (cell D in the table).

Table 3.   Schematic of the contingency table we used to verify our hindcasts of October SIC values for the Beaufort Sea. A represents the number of instances where AN was hindcasted and observed, B represents the number of instances where AN was hindcasted and BN was observed, C represents the number of instances where BN was hindcasted but AN was observed, and D represents the number of instances where BN was hindcasted and BN was observed. Note that a different contingency table for each lead time and each regression model, but all of them had the same form as the table shown here.

		OBSERVED	
		AN	BN
HINDCASTS	AN	A	B
	BN	C	D

From our contingency table results, we calculated four different verification metrics. The first is the percent correct (PC), which is simply the percent of forecasts that correctly predicted the subsequent event. PC is calculated as:

$$PC = \frac{A + D}{n} \qquad (1)$$

where n is the total number of hindcasts. In our study, n = 29 based on 29 years of data.

The second verification metric is false alarm rate (FAR). It quantifies the proportion of forecasts that are considered failures, so smaller FAR indicates better forecast performance. There are two FAR values that take into consideration AN and BN SIC occurrences. FAR is calculated as:

$$FAR = \frac{B}{A + B}, \text{ for AN} \qquad (2)$$

$$FAR = \frac{C}{C + D}, \text{ for BN} \qquad (3)$$

The third verification metric is probability of detection (POD). The POD is the fraction of instances when the forecasted event occurred. Like FAR, there are two POD values to consider both AN and BN SIC instances. POD is calculated as:

$$POD = \frac{A}{A + C}, \text{ for AN} \qquad (4)$$

$$POD = \frac{D}{D + B}, \text{ for BN} \qquad (5)$$

The fourth and final verification metric is the Heidke skill score (HSS). The HSS quantifies the skill after removing credit for accurate forecasts that could have been achieved by random forecasting. Random forecasts are the reference forecasts that the actual forecasts are measured. An HSS of one indicates perfect forecasts; HSS of zero indicates forecast that have no skill over the reference forecast; and HSS less than zero indicates forecasts that have less skill than the reference forecast. HSS is calculated by using this equation:

$$HSS = \qquad (6)$$

$$\frac{2(AD - BC)}{(A + C)(C + D) + (A + B)(B + D)}$$

Verifying with several metrics is more valuable than verifying with an individual metric, because multiple metrics provide a more complete assessment of forecast performance. For more information about the verification metrics used in this study, refer to Wilks (2006).

We used the following criteria to assess the hindcast performance of each regression model and to determine whether the predictors used in that model were viable (criteria adapted from Heidt (2009)).

1)   PC values greater than 0.5

2)   POD equal to or greater than FAR

3)   HSS values of 0.3 or greater

If all three criteria were met, we labeled the regression model as skillful and the predictors used in that model as viable predictors of October SIC in the Beaufort Sea.

D.   SUMMARY OF LONG RANGE FORECAST METHODS

Figure 14 is a flow chart of the set of processes used in this study to analyze climate variations and choose viable predictors of October SIC in the Beaufort Sea at lead times of several months. These processes use advanced atmospheric and oceanic reanalysis data, as well as advanced passive-microwave satellite based sea ice data. These processes include climate analyses using advanced statistical methods to identify climate patterns and processes that affect sea ice conditions. For this flow chart, October SIC in the Beaufort Sea is the predictand. But, the chart can be readily adapted for predictand periods and areas within the Arctic. Once the predictors are chosen at the end of this process, forecasts can be generated.
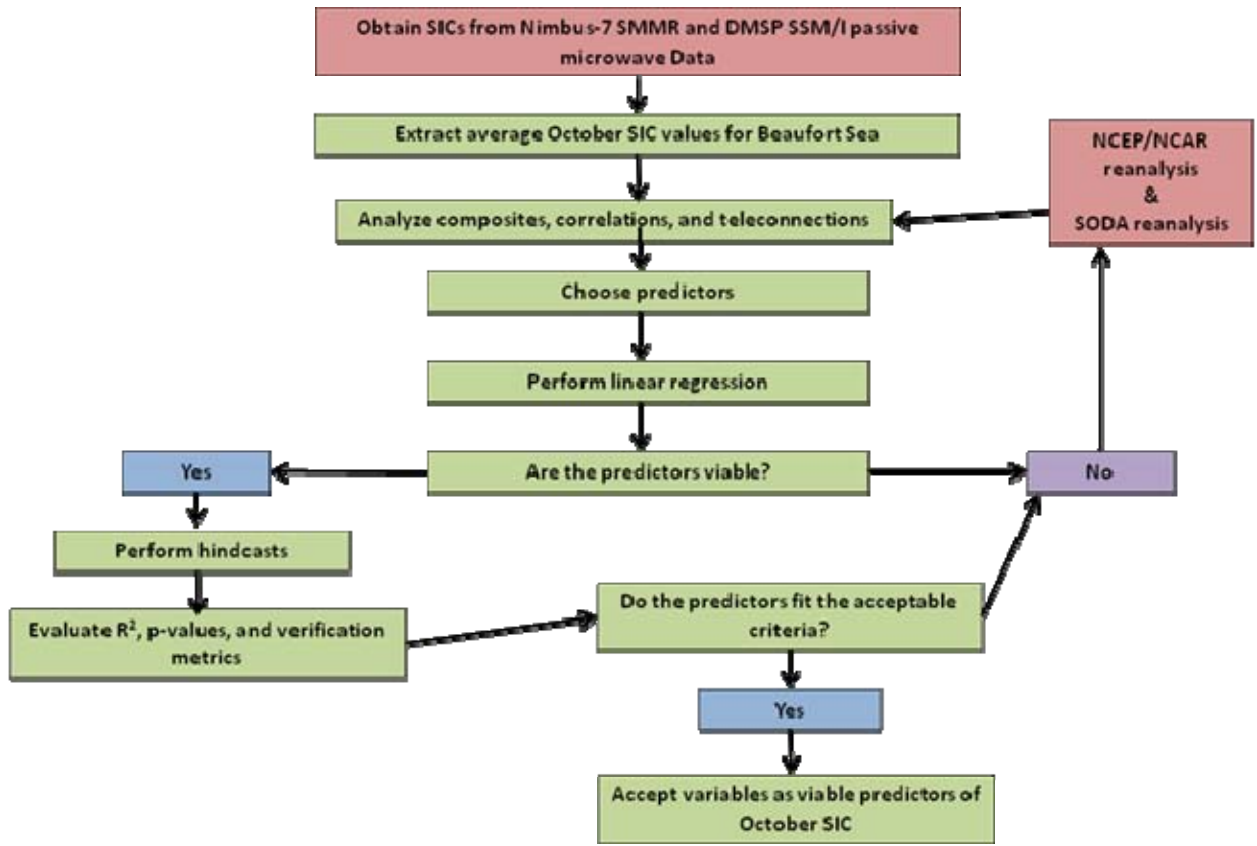
Figure 14.   Flow chart of the processes we used to identify predictors for use in developing and testing regression models for long-range forecasting of October SIC in the Beaufort Sea.

THIS PAGE INTENTIONALLY LEFT BLANK

III.   RESULTS

A.   ANALYSIS RESULTS

1.   Composite Analyses

To conduct our composite analyses, we constructed a time series of our predictand, October SIC in the Beaufort Sea, during 1979–2007 (Figure 15). This time series shows large interannual variations and a pronounced long term decline that is consistent with the corresponding results for other months for the Arctic as a whole (e.g., Figure 2).
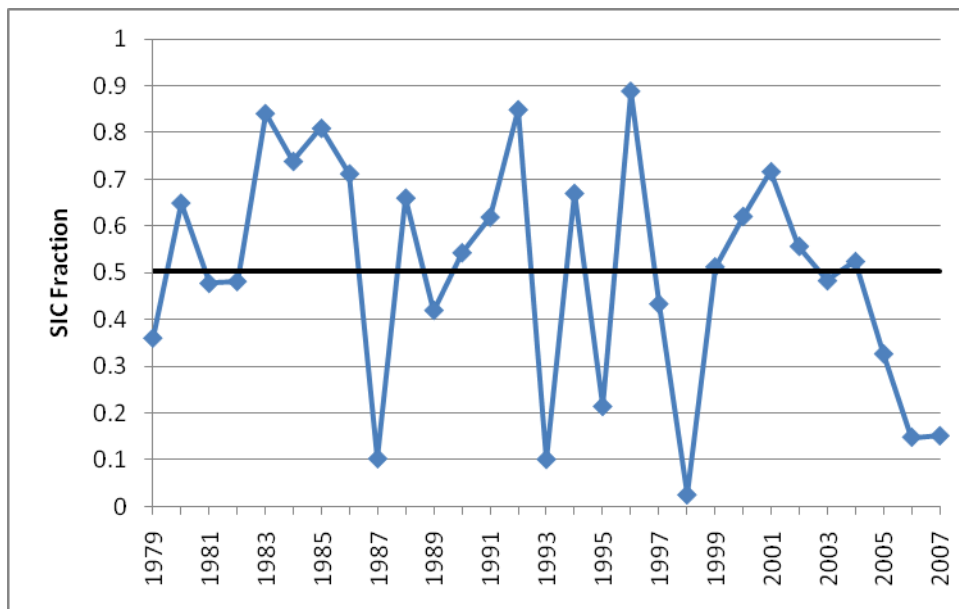
Figure 15.   Time series of our predictand, October SIC in the Beaufort Sea, during 1979–2007. The bold black line indicates the 1979–2007 LTM October SIC in our Beaufort Sea predictand region of 0.5047. Note the large interannual variations and long term downward trend.

From the predictand time series, we identified the five years with the most extreme high and low SIC values (Table 4). Both 2006 and 2007 were among the five extreme low SIC years. To get a more representative sample of low SIC years, we chose to replace 2006 with the sixth lowest year, 1995. The average of the high (low) SIC years is 1991 (1996, or 1998 if 2006 is used instead of

1995). This indicates that extremely high (low) SIC was more common earlier (later) in the study period. This result is consistent with the long term decline in SIC shown in Figure 15, and is important in selecting and evaluating base periods to use in calculating LTMs and anomalies associated with SIC extremes (see Chapter II, Section C.1, and the discussion of Figure 20).

Table 4.   Years selected to represent extreme high and low SIC in October in the Beaufort Sea.

Extreme High SIC Years	Extreme Low SIC Years
2001	2007
1996	1998
1992	1995
1985	1993
1983	1987

We used the high and low SIC years shown in Table 4 to construct composites of the atmospheric and oceanic conditions associated with high and low SIC in October in the Beaufort Sea. The composites were used to identify: (a) the major spatial and temporal patterns and dynamical processes lead to SIC variations; and (b) potential predictors of SIC variations (see Chapter II, Section C).

Figure 16a shows the LTM October SIC for the Beaufort Sea and nearby regions. The LTM SIC in October for our Beaufort Sea predictand region (Figure 8) is approximately 0.50. Figure 16b shows the October SIC composite mean for extreme high SIC years. The average SIC in October for our Beaufort Sea predictand region is approximately 0.82, which is a 64% increase from the LTM. Figure 16c shows the October SIC composite mean for the extreme low SIC years. The average SIC in October for our Beaufort Sea predictand region is approximately 0.12, which is a 76% decrease from the LTM. These substantial

deviations from the LTM SC value quantify the magnitude of the SIC anomalies that the Beaufort Sea can experience. They also highlight the scientific and operational importance of climate analyses and long-range forecasts of these anomalies.
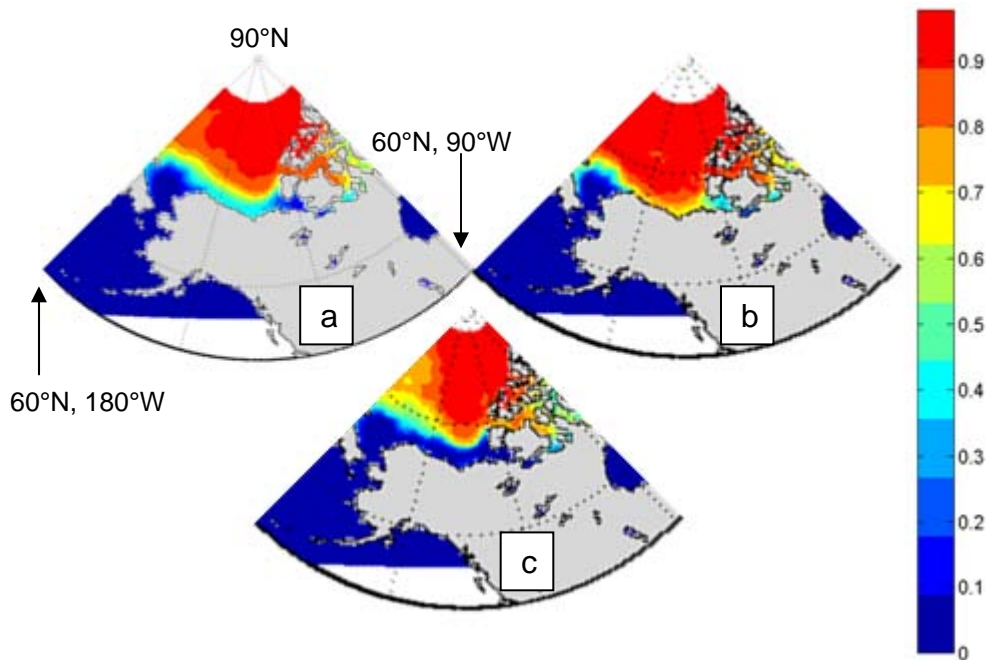
Figure 16.   Composites of October SIC in the Beaufort Sea and nearby regions for: (a) LTM; (b) the five extreme high SIC years in the Beaufort Sea; (c) the five extreme low SIC years in the Beaufort Sea. SIC in the Beaufort Sea in the extreme high (low) years was 64% (76%) greater (lower) than the LTM.

Figure 17 shows the 850 hPa GPH composite anomalies for the extreme high and low SIC years (Table 4). During years with high (low) SIC, there were: (a) below (above) average heights over the Beaufort Sea; (b) above (below) average heights over Siberia; and (c) below (above) average heights over northern central Russia. These findings are: (a) consistent with Barnett (1980); and (b) indicate that high (low) SIC in the Beaufort Sea in October tends to be associated with anomalously low (high) pressures and westerly (easterly) winds at low levels over the Beaufort Sea that are part of a pan-Arctic pattern of anomalous low level heights and winds.

43
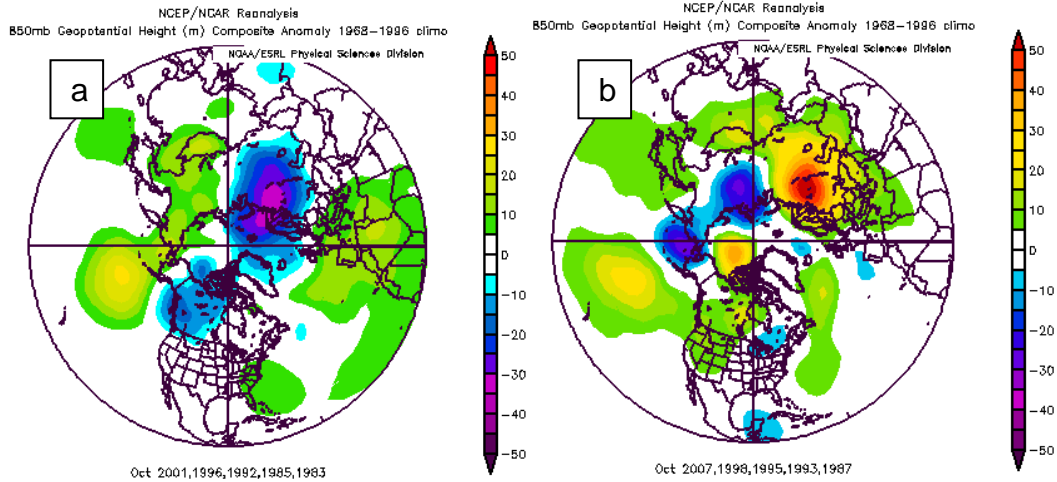
Figure 17.   Composite anomalies of October 850 hPa GPH (m) for: (a) the five extreme high SIC years in the Beaufort Sea and (b) the five extreme low SIC years in the Beaufort Sea. Note the generally negative (positive) anomalies in the Beaufort Sea region in the high (low) SIC years.

Figure 18 shows the corresponding surface vector wind composite anomalies for years of high and low SIC in the Beaufort Sea. For years with high (low) SIC, an anomalous cyclonic (anticyclonic) circulation is evident near the Beaufort Sea region, consistent with the 850 hPa GPH anomalies (Figure 17).
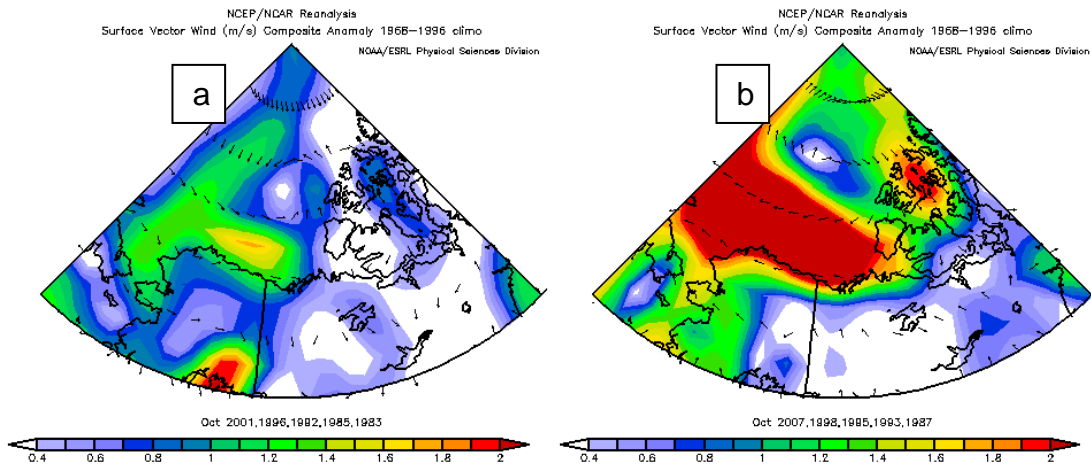
Figure 18.   Composite anomalies of October surface vector winds (m/s) for: (a) the five extreme high SIC years in the Beaufort Sea and (b) the five extreme low SIC years in the Beaufort Sea. Note the generally cyclonic (anticyclonic) anomalies in the Beaufort Sea region in the high (low) SIC years.

Figure 19 shows the surface air temperature composite anomalies for the extreme high and low SIC years. For years with high (low) SIC, there were below (above) average air temperatures in the vicinity of the Beaufort Sea. These results are physically plausible, since below (above) average air temperatures would tend to accelerate (inhibit) sea ice growth in the region.
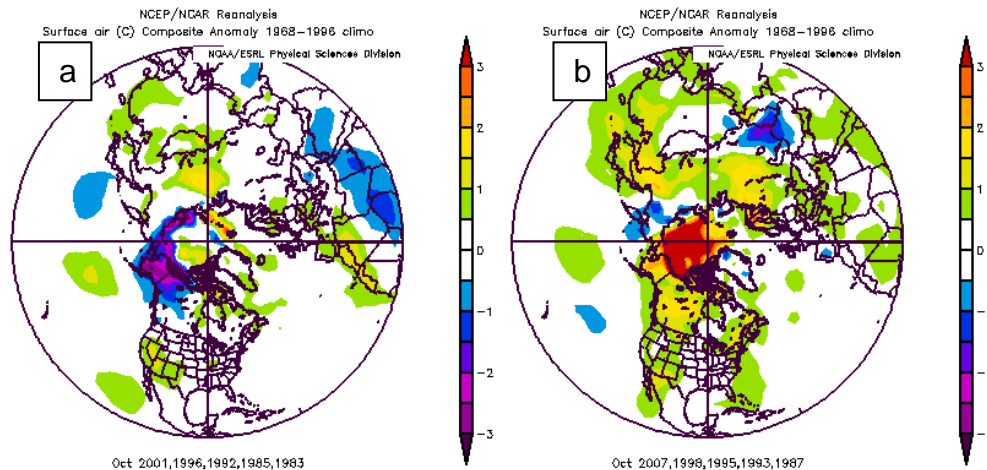
Figure 19. Composite anomalies of October surface air temperature (°C) for: (a) the five extreme high SIC years in the Beaufort Sea and (b) the five extreme low SIC years in the Beaufort Sea. Note the generally negative (positive) anomalies in the Beaufort Sea region in the high (low) SIC years.

Figure 20 shows the 5 m ocean temperature composite anomalies for extreme high and low SIC years in October in and near the Beaufort Sea. Upper ocean temperatures were below (above) average in the Beaufort Sea during years with high (low) sea ice. The 5 m ocean temperature composite anomalies are similar to those at other levels in the upper 50 m (not shown). The high SIC composite shows temperature anomalies that are only slightly negative, while the low SIC composite shows temperature anomalies that are quite positive. This may be a result of our use of the 1968–1996 base period for calculating anomalies (see Chapter II, Section C.1, and discussion of Table 4, above). This base period begins and ends about ten years before our 1979–2007 study period. Long term warming of the upper ocean in the Arctic during recent years could mean that our base period represents a cooler period than our study period. If so, then our ocean temperature anomalies would tend to be positively

45

biased. Figure 19 shows some hints of a positive bias in the air temperature anomalies as well. This indicates that additional research on long term trends in oceanic and atmospheric temperatures in the Arctic is needed.
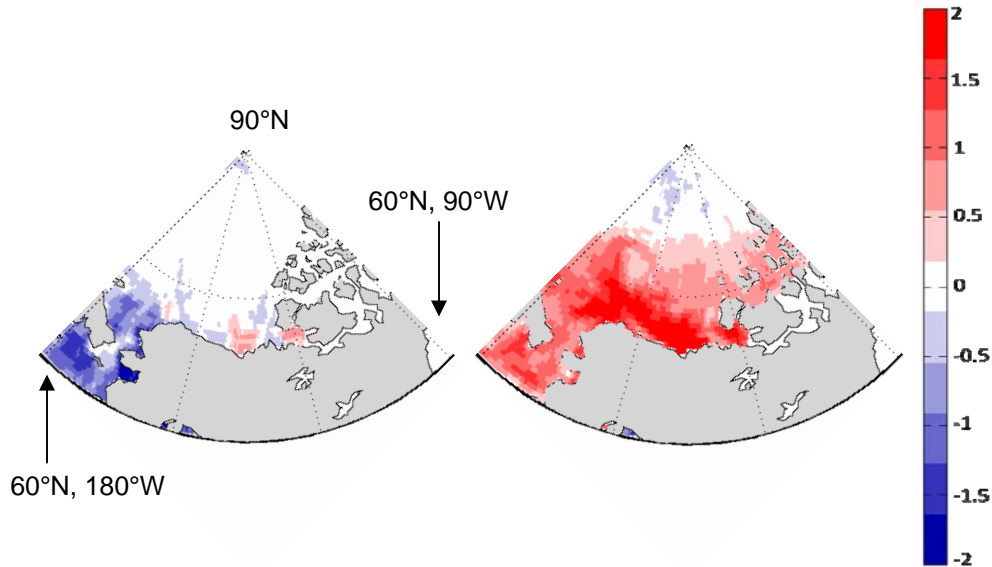
Figure 20.   Composite anomalies of October 5 m ocean temperature (°C) for: (a) the five extreme high SIC years in the Beaufort Sea and (b) the five extreme low SIC years in the Beaufort Sea. Note the generally negative (positive) anomalies in the Beaufort Sea region in the high (low) SIC years.

Figure 21 shows the high and low SIC composite anomalies of ocean currents averaged over the upper 5–57 m in the Beaufort Sea and nearby regions. The anomalous circulation patterns are not distinct except for an anomalous cyclonic (anticyclonic) circulation in the western Beaufort Sea high (low) SIC composite, indicated by the bold black schematic arrows.
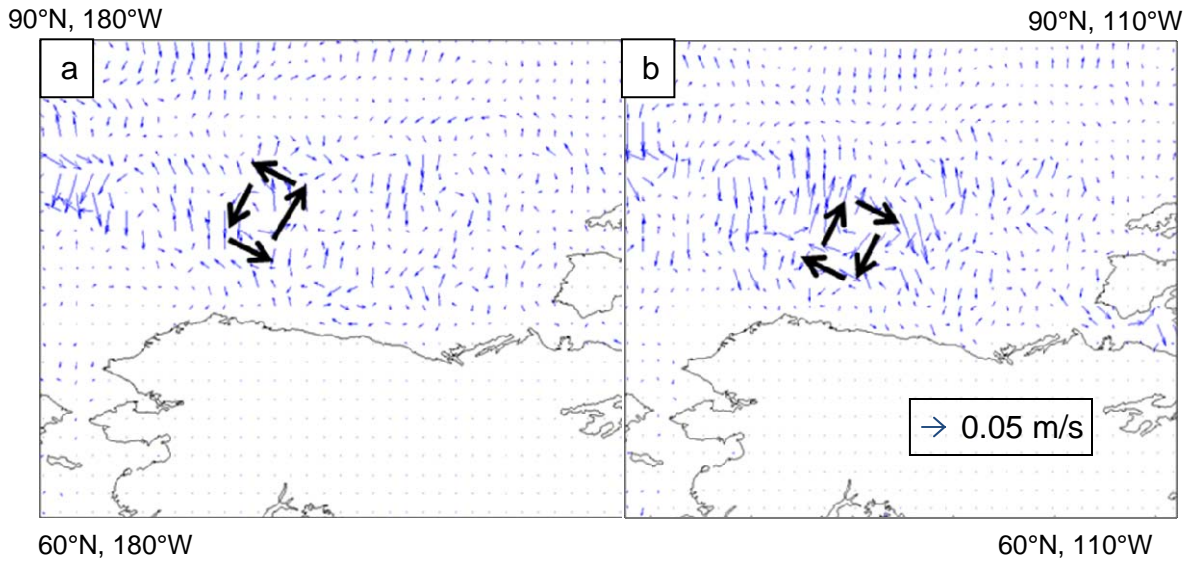
Figure 21. Composite anomalies of October ocean current (m/s) averaged over 5 to 57 m for: (a) the five extreme high SIC years in the Beaufort Sea and (b) the five extreme low SIC years in the Beaufort Sea. Black arrows schematically show the direction of anomalous circulations in the western Beaufort Sea where there are generally cyclonic (anticyclonic) anomalies in the high (low) SIC composite.

In summary, our composite analyses revealed several characteristic anomalies associated with extremely high (low) SIC in October in the Beaufort Sea (BS): (a) anomalously low (high) heights and westerly (easterly) winds at low levels over and to the west of the BS; (b) anomalously warm (cool) surface air temperatures over and near the BS; and (c) anomalously warm (cool) upper ocean temperature in and near the BS; (d) cyclonic ocean currents in the western BS. These height and wind anomalies are consistent with prior studies (e.g., Barnett 1980); the temperature anomalies are consistent with the SIC extremes; and the current anomalies are broadly consistent with the wind anomalies. These results suggest that there are relatively consistent and dynamically understandable patterns and processes associated with extremes in SIC in the BS. These results are encouraging because they indicate that statistical and dynamical climate analyses, and long-range forecasting methods, have the potential to improve long-range operational support.

2. Correlations and Teleconnections

We conducted correlation analyses to identify relationships between our predictand (October SIC in the Beaufort Sea, Figure 15) and a wide range of potential predictors, with the potential predictors leading by zero to five months. The potential predictors were globally distributed climate system variables (e.g., global SST, global 200 hPA GPH, global 850 hPa GPH; AOI, NAOI, MEI, SOI, PNAI). These correlation analyses resulted in a series of maps showing the correlation between our predictand and the potential predictors. Correlations that were strong and persistent correlations at all lead times were selected for further statistical and dynamical analyses. Only some of these correlation results are shown in this report. See Chapter II, Section C, for more information on our correlation methods and the interpretation of our correlation results.

One of the focus variables for our correlation analyses was SST. This is because: (a) climate variations in the ocean tend to be relatively persistent; (b) climate variations in the atmosphere are relatively sensitive to small changes in SST; (c) teleconnections can allow SST variations in one location to significantly impact atmospheric and oceanic conditions in very distant locations; and (d) SST data is readily available in near real time, which means SST is a feasible predictor for use in LRF systems (van den Dool 2007; Murphree 2008b).

We correlated our predictand time series (Figure 15) with global SSTs for 1979–2007, with SSTs leading by one to five months. These correlations allowed us to assess how SST variations around the globe might contribute to variations in October SIC in the Beaufort Sea in October via teleconnection processes.

Figure 22 shows the maps of the correlations between October SIC in the Beaufort Sea and global SSTs, with SST leading by one, three, and five months. At all lead times, there are significant negative correlations at all leads with SSTs in the Caribbean Sea region, with the strength of the correlation increasing with lead time. There is also evidence of weaker but still significant negative correlations with SSTs in the vicinity of the Icelandic Low, primarily at the shorter

48

leads. The correlations with tropical Pacific SST are relatively weak and non-persistent, with spatial patterns that are only vaguely consistent with ENLN patterns. There is also a significant negative correlation with tropical Indian SST at a five month lead. The negative correlations mean that when SST increases (decreases), October SIC in the BS tends to decrease (increase) one to five months later.

In the North Atlantic, Figure 22 shows evidence of a tripole pattern (especially at a five month lead), with negative correlations in the tropics and subpolar North Atlantic, and positive correlations in the midlatitude North Atlantic. This pattern is similar to the tripole (and quadripole) patterns in SST anomalies associated with the NAO and AO (Murphree 2008c), and suggests that the NAO and AO may play a role in establishing these correlations and teleconnections.

The strengthening of correlations as lead time increases (e.g., for SST in the Caribbean Sea) is an especially interesting result, since it indicates the potential for enhanced predictability and skillful LRFs at longer leads.
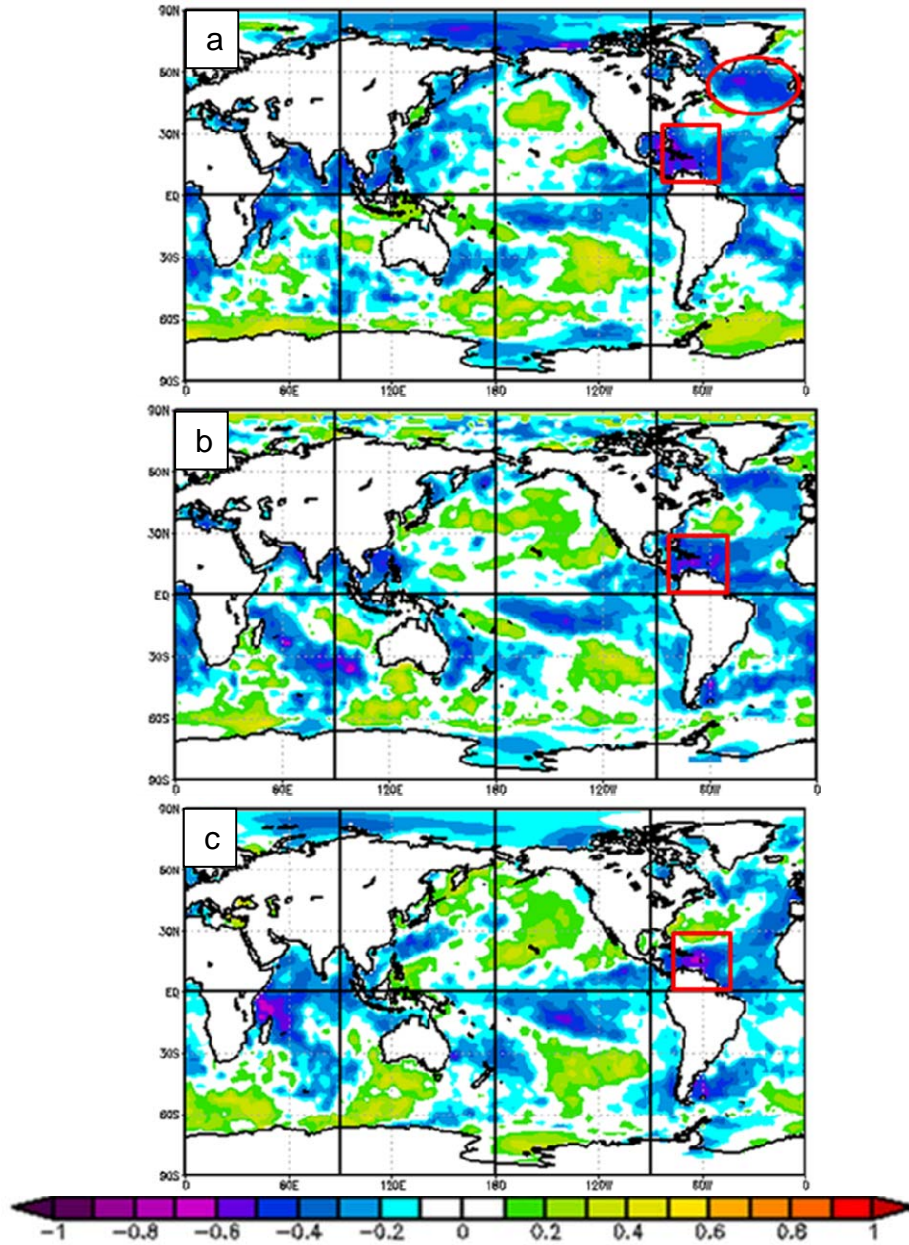
Figure 22. Map of correlations between October SIC in the Beaufort Sea and global SSTs, with SST leading by: (a) one month; (b) three months; and (c) five months. Negative (positive) correlations indicate that when October SIC is high, SST tends to be low (high). Correlations with magnitudes ≥ 0.363 are significant at the 95% level (see Chapter II, Section C.2). At all leads, there is a significant negative correlation with the SSTs in the Caribbean Sea (red box). At shorter leads, there is a significant negative correlation with the SSTs south of Iceland (red oval).

3. Predictor Selection

Based on our correlation results, we identified SST in the Caribbean region as a potential predictor. Similar types of correlation results (not shown) led us to identify several other potential predictors in the Beaufort Sea region, and in regions from the Beaufort Sea, including: (a) surface air temperature near Alaska and northwest (NW) Canada; (b) surface air temperature near Iceland; and (c) geopotential height (Z) at 850 hPa near Iceland.

Table 5 lists the variables that we tested as potential predictors of October SIC in the Beaufort Sea at lead times of one to five months. The potential predictors marked with *BS* were all area averaged quantities for the Beaufort Sea region shown in Figure 8. The other predictors were also area averaged quantities but for the other regions shown in the right column of Table 5. These regions were: Alaska (AK), northwest Canada (NW), region of the Icelandic low region (IC), and the Caribbean Sea (CS). The exact locations of these regions are stated in Table 5 and the approximate locations are shown in Figure 23.

Table 5. The variables tested as potential predictors of October SIC in the Beaufort Sea at lead times of one to five months. The variables were averaged within the defined boxes shown in Figure 23 and then tested as possible predictors by means of a linear regression. BS indicates for Beaufort Sea. SIC BS indicates SIC in the BS at a lead of one to five months prior to the October predictand period.

Potential Predictors of October SIC	Variable Location
Z 850 hPa BS	80°-82.5°N, 142.5°-127.5°W
u winds surface BS	70°-72.5°N, 148°-127.5°W
v winds surface BS	70°-72.5°N, 148°-127.5°W
ocean temperatures 5 m BS	70°-72.5°N, 148°-127.5°W
u ocean currents 5-57 m BS	70°-72.5°N, 148°-127.5°W
v ocean currents 5-57 m BS	70°-72.5°N, 148°-127.5°W
SIC BS	70°-72.5°N, 148°-127.5°W
T surface air Alaska/NW Canada/BS	BS: 70°-72.5°N, 148°-127.5°W
	AK: 62.5°-67.5°N, 147.5°-132.5°W
	NW: 50°-52.5°N, 126°-117.5°W
SST Caribbean Sea (CS)	10°-22°N, 64°-76°W
Z 850 hPa Icelandic Low (IC)	55°-57.5°N, 45°-30°W
T surface air Icelandic Low (IC)	55°-57.5°N, 45°-30°W
Climate variation indices (AO, NAO, PNA, MEI, SOI, Nino 3.4)	See main text.
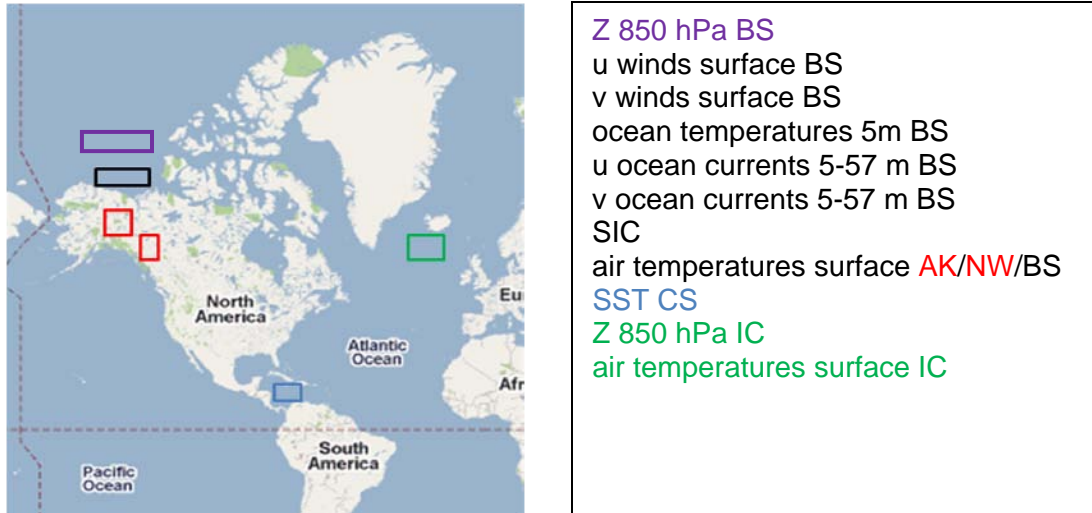
Figure 23.   Approximate locations of variables tested as predictors of October SIC. Colors of the boxes correspond to colors of variables listed in the legend.

The variables listed in Table 5 were tested via linear regression as potential predictors of SIC in October in the Beaufort Sea (our predictand) at lead times of one to five months. For each lead time, we ranked the predictors by their R^2. Tables 6 through 10 display the results of these linear regressions at all lead times of five months to one month, respectively.

Table 6.   R and R^2 obtained when performing linear regressions between our predictand (SIC in October in the Beaufort Sea) and the May values of the listed variables (five month lead time). The variables are ranked by their R^2 values (highest R^2 listed first).

Variable	R	R^2
T surface air NW	-0.6159	0.379333
SST CS	-0.533	0.284089
SIC BS (May)	0.50233	0.252335
ocean temperature 5 m BS	-0.4506	0.20304
u winds surface BS	0.370798	0.137491
Z 850 hPa BS	-0.3449	0.118956
T surface air IC	-0.31938	0.102001
NAO	0.279922	0.078356
Nino 3.4	-0.23265	0.054126
MEI	-0.20975	0.043995
Z 850 hPa IC	-0.14728	0.02169
AO	0.125407	0.015727
v wind surface BS	0.115744	0.013397
v ocean current 5-57 m BS	0.08294	0.006879
PNA	0.072001	0.005184
u ocean current 5-57 m BS	0.03584	0.001284
SOI	0.003094	9.57E-06

Table 7.   R and R^2 obtained when performing linear regressions between our predictand (SIC in October in the Beaufort Sea) and the June values of the listed variables (four month lead time). The variables are ranked by their R^2 values (highest R^2 listed first).

Variable	R	R^2
SIC BS (June)	0.642289	0.412536
SST CS	-0.54686	0.299057
T surface air IC	-0.46522	0.216431
Z 850 hPa BS	-0.4647	0.215946
ocean temperature 5 m BS	-0.46204	0.213484
NAO	0.434258	0.18858
u wind surface BS	0.42164	0.17778
AO	0.312127	0.097423
v wind surface BS	0.266371	0.070954
Nino 3.4	-0.22073	0.048722
Z 850 hPa IC	0.193182	0.037319
T surface air BS	-0.15276	0.023337
MEI	-0.1505	0.02265
PNA	0.049223	0.002423
SOI	-0.03249	0.001056
v ocean current 5-57 m BS	0.011978	0.000143
u ocean current 5-57 m BS	0.001093	1.19E-06

Table 8.   R and R^2 obtained when performing linear regressions between our predictand (SIC in October in the Beaufort Sea) and the July values of the listed variables (four month lead time). The variables are ranked by their R^2 values (highest R^2 listed first).

Predictors	R	R^2
SIC BS (July)	0.72136	0.52036
SST CS	-0.5649	0.319112
Z 850 hPa BS	-0.4614	0.21289
ocean temperature 5 m BS	-0.45699	0.208835
T surface air IC	-0.44125	0.1947
u wind surface BS	0.439249	0.19294
T surface air BS	-0.37935	0.143909
NAO	0.332359	0.110463
AO	0.280684	0.078784
PNA	-0.26557	0.070527
Nino 3.4	-0.19753	0.039018
v ocean current 5-57 m BS	0.186886	0.034926
MEI	-0.14404	0.020748
v wind surface BS	0.096455	0.009304
Z 850 hPa IC	-0.07954	0.006327
u ocean current 5-57 m BS	0.074672	0.005576
SOI	0.056746	0.00322

Table 9.   R and R^2 obtained when performing linear regressions between our predictand (SIC in October in the Beaufort Sea) and the August values of the listed variables (two month lead time). The variables are ranked by their R^2 values (highest R^2 listed first).

Predictors	R	R^2
SIC BS (August)	0.75357	0.567868
T surface air IC	-0.7145	0.51051
SST CS	-0.5573	0.310583
Z 850 hPa IC	-0.4985	0.248502
T surface air BS	-0.48568	0.235882
ocean temperature 5 m BS	-0.46406	0.215355
Z 850 hPa BS	-0.35254	0.124287
v wind surface BS	0.30617	0.09374
AO	0.288654	0.083321
NAO	0.252233	0.063621
PNA	-0.24495	0.060001
SOI	0.24244	0.058777
u wind surface BS	0.192517	0.037063
MEI	-0.16505	0.027242
Nino 3.4	-0.16274	0.026484
u ocean current 5-57 m BS	0.036114	0.001304
v ocean current 5-57 m BS	0.034264	0.001174

Table 10. R and R^2 obtained when performing linear regressions between our predictand (SIC in October in the Beaufort Sea) and the September values of the listed variables (one month lead time). The variables are ranked by their R^2 values (highest R^2 listed first).

Predictors	R	R^2
SIC BS (September)	0.7407	0.548636
T surface air AK	-0.721	0.519841
SST CS	-0.5097	0.259794
u wind surface BS	0.483429	0.233704
ocean temperature 5 m BS	0.468156	0.21917
T surface air IC	-0.4471	0.199898
Z 850 hPa BS	-0.3969	0.15753
v ocean current 5-57 m BS	0.288897	0.083461
PNA	-0.28132	0.079141
u ocean current 5-57 m BS	0.233393	0.054472
Z 850 hPa IC	0.144475	0.020873
MEI	-0.13375	0.017889
Nino 3.4	-0.13115	0.0172
AO	-0.0949	0.009006
SOI	0.079489	0.006319
NAO	-0.02031	0.000412
v wind surface BS	0.016231	0.000263

The results from the linear regressions (Tables 6-10) show that there are predictand-predictor pairs with high R^2 values at all lead times. The predictors with the overall highest R^2 values for all lead times are shown in Table 11. This summary of the regression based rankings of the potential predictors indicates highlights two variables potentially important predictors over all leads: (a) SIC in the Beaufort Sea (SIC BS) one to five months prior to the predictand period (October); and (b) SST in the Caribbean Sea region (SST CS) one to five months prior to the predictand period (October). Other variables have higher R^2 values at some leads (e.g., T AK at a lead of one month). But, Table 11 indicates that SIC BS and SST CS would be a useful predictor pair at all leads.

Table 11. Summary of the variables that showed a high R^2 value for all linear regressions at all lead times. The symbols for the variables are explained in the main text for Table 5. The numbers in the variable columns indicate the R^2 rank for the indicated variable and lead time (see Tables 6-10). The parenthetical terms indicate the circulation variable with the high R^2 rank (Z, U. v) or T.

Lead Time (months)	Predictor Variables with Overall Highest R^2 Values					
	SIC BS	SST CS	Circulation (Z, u, v) BS	T air sfc AK/NW/BS	T ocean 5m BS	Circulation or T (Z, T sfc air) IC
5	3	2	5 (u)	1	4	---
4	1	2	4 (Z)	3	5	---
3	1	2	3 (Z)	---	4	5 (T)
2	1	3	7 (v)	5	6	2 (T) 4 (Z)
1	1	3	4 (u)	2	5	6 (T)

Our goal was to develop hindcasts of October SIC at all lead times based on the optimal combination of predictors. Based on the results in Table 11, we developed the four different predictor combination sets shown in Table 12. Predictor set 1 includes SIC BS and SST CS. Predictor set 2 is the same as predictor set 1 but with 5 m ocean T added. Predictor set 3 is the same as predictor set 2 but with Z 850 hPa BS added. Predictor set 4 represents several special cases in which based on additions to or subtractions from the predictors used in sets 1-3. We used predictor sets 1-4 to generate hindcasts for 1979-2007 of our predictand (SIC in October in the Beaufort Sea).

Table 12. Four predictor sets developed and tested via hindcasts for 1979–2007 of October SIC in the Beaufort Sea.

Predictor set 1	Predictor set 2	Predictor set 3	Predictor set 4
• SIC BS • SST CS	• SIC BS • SST CS • T 5 m BS	• SIC BS • SST CS • T 5 m BS • Z 850 hPa BS	• Special cases

B.   HINDCAST AND VERIFICATION RESULTS

Figures 24–32 and Tables 13–17 summarize our hindcast results when using the predictor sets shown in Table 12. These figures show, for different lead times, time series of the hindcast results (blue curve) and the observed SIC (red curve), along with the LTM October SIC (bold black line). For verification of the hindcasts, the SIC hindcasted and observed SIC values for each year were designated as above (below) average, if the SIC was above (below) the LTM SIC amount of 0.50.

1.   Predictor Set 1

Figures 24 shows the observed and hindcasted SIC time series for October 1979–2007, with the hindcasts based on linear regression at a 5-month lead time and using predictor set 1 (SIC BS in May and SST CS in May). Table 13 shows the corresponding contingency table and verification results. The figure shows a good overall visual agreement between the hindcasts and observed SIC, with some years being especially well hindcasted (e.g., most of the years during 1994–2004). There are however some notable examples of over and under hindcasting (e.g., 1983, 1987, 1991, 1993, 2006, 2007). Both the AN and BN POD values are larger than the AN and BN FAR values, and the HSS is greater than 0.3 which are all acceptable based on our set of hindcast performance criteria (see Chapter II, Section C.5.b). The criteria set for an acceptable PC value was greater than 0.7, and the PC in this case was slightly below the acceptable limit. The R^2 value was 0.423018, the p-value for Caribbean SSTs was 0.003543, and the p-value for the Beaufort Sea SIC was 0.006537. Both p-values were acceptable and indicate statistical significance.

The model over predicted the SIC in October 2006 at lead times of five, four, and three months. This was due to the atypical relationship that SIC in October 2006 had with the SIC in previous months of 2006. As shown in Tables 6 through 11, SIC in previous months has a strong and consistent positive correlation with SIC in October at all lead times. So, when higher than average

60

values of SIC in the Beaufort Sea is observed in earlier months, the regression model will predict above average SIC in October. 2006 was an atypical year in which SIC in the Beaufort Sea was higher than normal in May, June, and July (not shown), but was below normal in October. Thus, the regression model based on the May, June, and July 2007 SIC predictors over-predicted the October SIC. Apparently, one or more processes occurred in spring-Summer 2006 that caused the sea ice in the Beaufort Sea to melt at a much faster rate than normal, resulting in below average SIC in October. Further research is needed to identify and conclude what other mechanisms occurred to accelerate the melting that occurred in 2006.
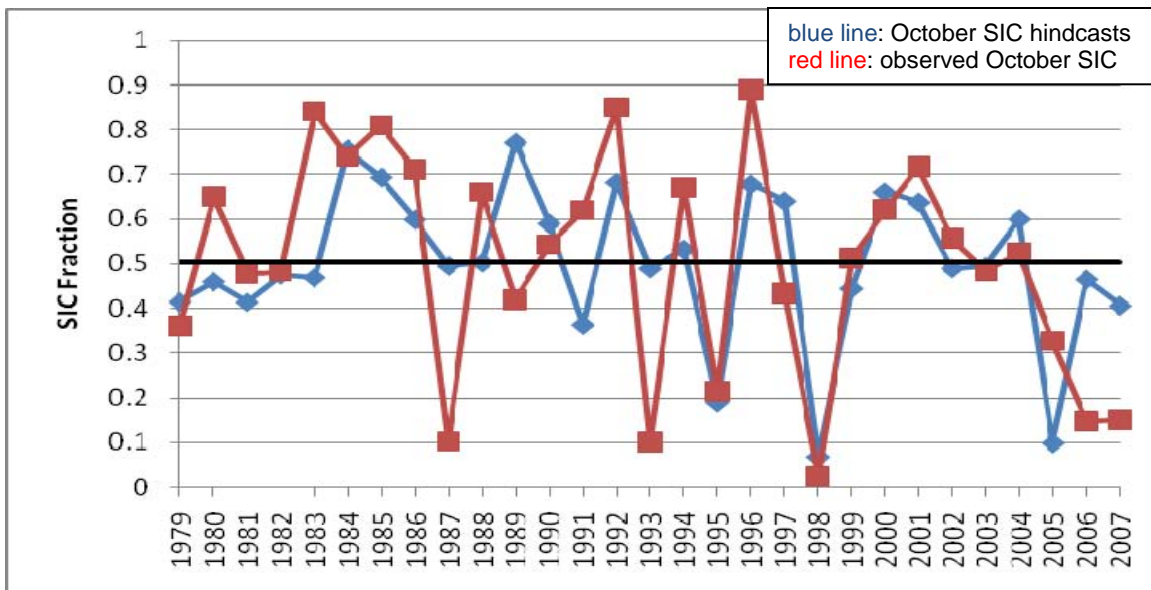
Figure 24. Time series of observed (red) and five-month lead hindcasted (blue) October SIC in the Beaufort Sea for 1979–2007. Hindcasts are based on linear regression using predictor set 1 values from the preceding May. See Table 12 for predictor set 1 variables. The R^2 value was 0.423018. The p-value for Caribbean SSTs was 0.003543, and the p-value for the Beaufort Sea SIC was 0.006537. The bold black line indicates the 1979–2007 LTM October SIC in our Beaufort Sea predictand region of 0.5047.

Table 13. Contingency table and verification results for five-month lead
hindcasts of October SIC in the Beaufort Sea for 1979–2007. Hindcasts
are based on linear regression using predictor set 1 variables. See
Chapter II, Section C, 5, for explanations of the contingency table and the
verification metrics shown in this table.

Verification of predictor set 1 five-month lead hindcasts			
		OBSERVED	
		AN	BN
HINDCASTS	AN	7	4
	BN	6	12
MAE		0.15	
RMSE		0.19	
PC		0.66	
FAR (AN)		0.36	
FAR (BN)		0.33	
POD (AN)		0.54	
POD (BN)		0.75	
HSS		0.35	

Figure 25 shows the time series of the hindcasts of October 1979-2007
SIC using predictor set 1 at a lead time of four months, along with the actual
October 1979–2007 SIC values. Like the five month lead hindcasts (Figure 24),
the four month lead hindcasts predict the SIC from 1994 to 2004 more accurately
than other years. The problems in predicting the 2006 SIC are also similar to
those for the five month lead hndcasts, for the reasons previously stated. Table
14 shows the corresponding contingency table and verification results. The R^2
value was 0.42811, the p-value for Caribbean SSTs was 0.108507, and the p-
value for the Beaufort Sea SIC was 0.007782. The R^2 value was greater than for
the five month lead hindcasts (Figure 24) and the p-values remained acceptable.
The AN and BN POD values were both greater than the AN and BN FAR values,

and the HSS value was greater than 0.3, making them all within the acceptable criteria. The PC value was approximately 0.01 below the acceptable PC criteria that we set forth. This difference was negligibly small, so we deemed this to be an acceptable PC value.
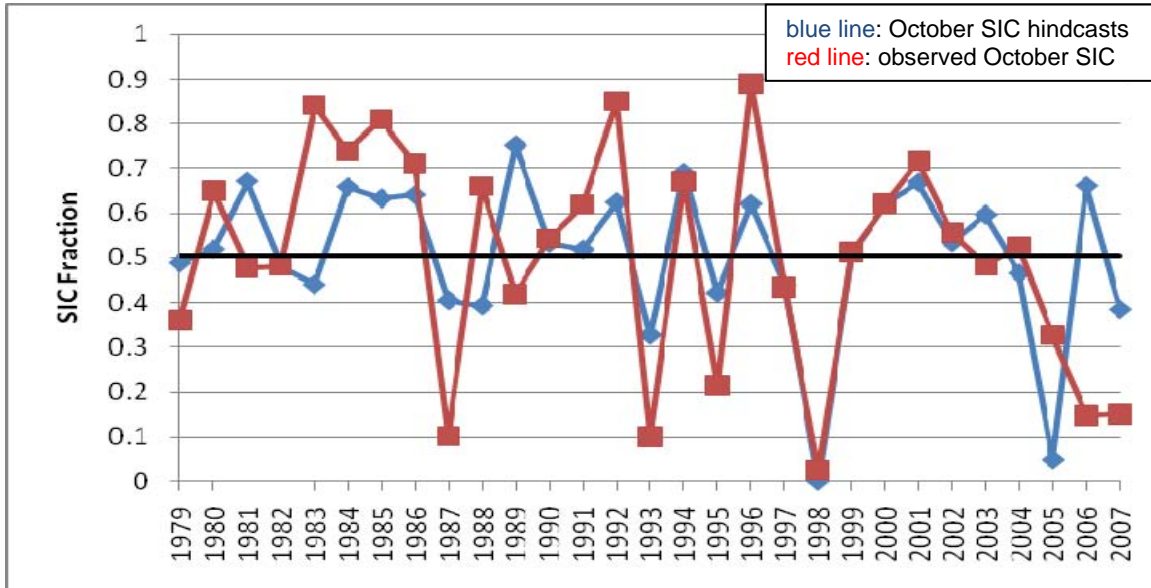
Figure 25.   Time series of observed (red) and four-month lead hindcasted (blue) October SIC in the Beaufort Sea for 1979–2007. Hindcasts are based on linear regression using predictor set 1 values from the preceding June. See Table 12 for predictor set 1 variables. The R^2 value was 0.42811. The p-value for Caribbean SSTs was 0.108507, and the p-value for the Beaufort Sea SIC was 0.007782. The bold black line indicates the 1979-2007 LTM October SIC in our Beaufort Sea predictand region of 0.5047.

Table 14. Contingency table and verification results for four-month lead hindcasts of October SIC in the Beaufort Sea for 1979–2007. Hindcasts are based on linear regression using predictor set 1 variables. See Chapter II, Section C,5, for explanations of the contingency table and the verification metrics shown in this table.

Verification of predictor set 1 four-month lead hindcasts			
		OBSERVED	
		AN	BN
HINDCASTS	AN	8	4
	BN	5	12
MAE			0.15
RMSE			0.20
PC			0.69
FAR (AN)			0.33
FAR (BN)			0.29
POD (AN)			0.62
POD (BN)			0.75
HSS			0.42

The three-month lead time hindcasts for October 1979-2007 SIC in the Beaufort Sea using predictor set 1 are shown in Figure 26, along with the actual October 1979-2007 SIC values. The model was able to follow the general trends and variations in sea ice very well throughout the whole time period, with the exception once again of 2006. Table 15 shows the corresponding contingency tables and verification results. All the metrics met our criteria. The R^2 value was 0.539094, the p-value for Caribbean SSTs was 0.088187, and the p-value for the Beaufort Sea SIC was 0.000576. The R^2 value was notably higher than for the five and four month lead hindcasts (Figures 24 and 25), and the p values for both predictors were acceptable.

64
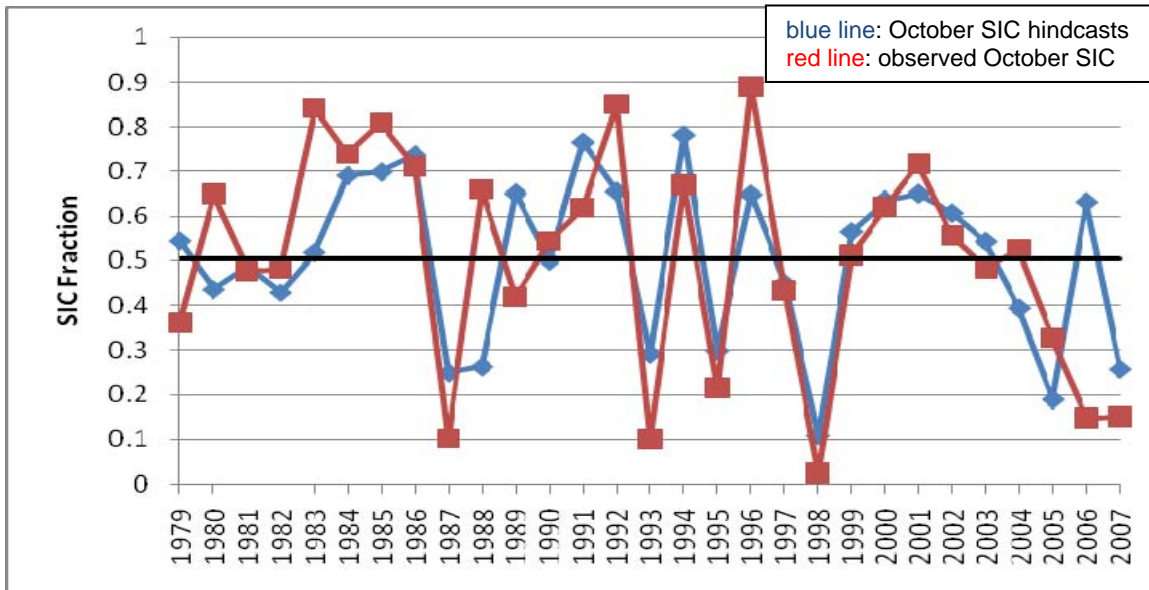
Figure 26.   Time series of observed (red) and three-month lead hindcasted (blue) October SIC in the Beaufort Sea for 1979–2007. Hindcasts are based on linear regression using predictor set 1 values from the preceding July. See Table 12 for predictor set 1 variables. The R^2 value was 0.539094. The p-value for Caribbean SSTs was 0.088187, and the p-value for the Beaufort Sea SIC was 0.000576. The bold black line indicates the 1979–2007 LTM October SIC in our Beaufort Sea predictand region of 0.5047.

Table 15. Contingency table and verification results for three-month lead hindcasts of October SIC in the Beaufort Sea for 1979–2007. Hindcasts are based on linear regression using predictor set 1 variables. See Chapter II, Section C, 5, for explanations of the contingency table and the verification metrics shown in this table.

Verification of predictor set 1 three-month lead time hindcasts			
		OBSERVED	
		AN	BN
HINDCASTS	AN	10	3
HINDCASTS	BN	3	13
MAE		0.14	
RMSE		0.18	
PC		0.79	
FAR (AN)		0.23	
FAR (BN)		0.19	
POD (AN)		0.77	
POD (BN)		0.81	
HSS		0.60	

The October 1979–2007 SIC hindcast results using predictor set 1 at a two month lead time are shown in Figure 27 along with the actual October SIC values. Table 16 shows the corresponding contingency table and verification results. The visual match between the hindcasted and observed values is similar to the match at longer leads. However, there were some notable examples of unrealistic interannual variations in the two month hindcasts that were not present in the longer lead hindcasts (e.g., variations in the two month hndcasts that were too large in 1985 and 1991, and too small in 1998–2001). The 2006 hindcast errors are smaller than those at longer leads. Figure 27 provides evidence that the overall performance for 1979–1995 was better at two month leads than at longer leads. The R^2 value was 0.578741, the p-value for

Caribbean SSTs was 0.110975, and the p-value for the Beaufort Sea SIC was 8.63E-05. All verification metrics were within the acceptable ranges.
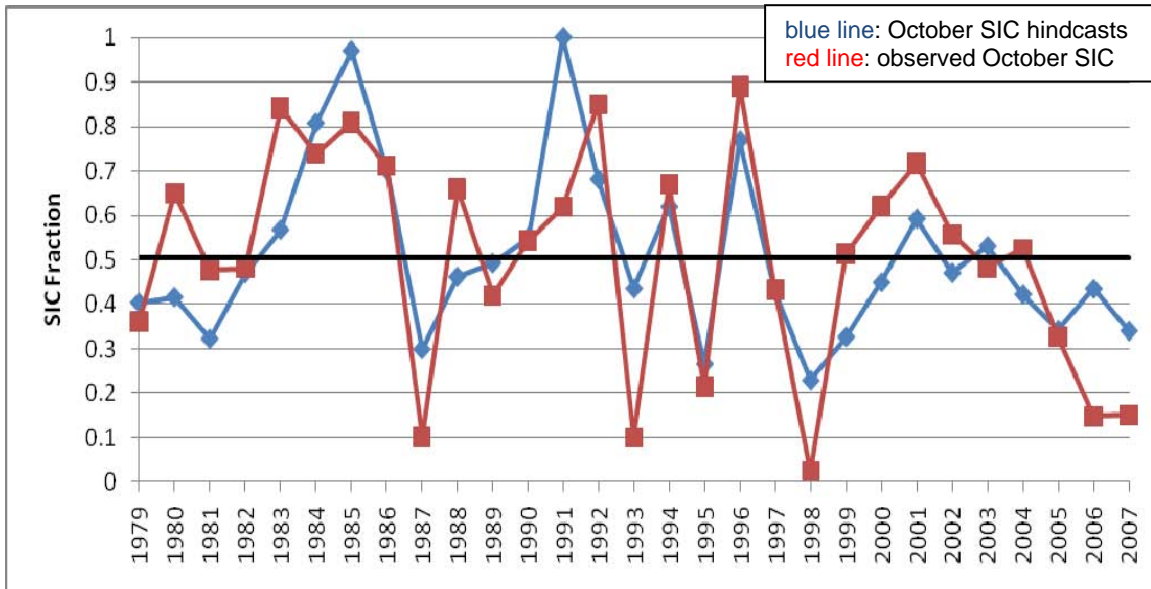

Figure 27. Time series of observed (red) and two-month lead hindcasted (blue) October SIC in the Beaufort Sea for 1979–2007. Hindcasts are based on linear regression using predictor set 1 values from the preceding August. See Table 12 for predictor set 1 variables. The R^2 value was 0.578741. The p-value for Caribbean SSTs was 0.110975, and the p-value for the Beaufort Sea SIC was 8.63E-05. The bold black line indicates the 1979-2007 LTM October SIC in our Beaufort Sea predictand region of 0.5047.

Table 16. Contingency table and verification results for two-month lead hindcasts of October SIC in the Beaufort Sea for 1979–2007. Hindcasts are based on linear regression using predictor set 1 variables. See Chapter II, Section C, 5, for explanations of the contingency table and the verification metrics shown in this table.

Verification of predictor set 1 two-month lead time			
		OBSERVED	
		AN	BN
HINDCASTS	AN	9	1
	BN	4	15
MAE		0.14	
RMSE		0.17	
PC		0.83	
FAR (AN)		0.1	
FAR (BN)		0.21	
POD (AN)		0.69	
POD (BN)		0.94	
HSS		0.65	

The results from the October 1979–2007 SIC hindcasts using predictor set 1 at a one-month lead time are shown in Figure 28, along with the actual October SIC values. The hindcasts show a notable overall improvement over those at longer leads, with the exception of the hindcasts for 2000–2002. Table 17 shows the contingency table and verification results. The R^2 value was 0.604912, the p-value for Caribbean SSTs was 0.021473, and the p-value for the Beaufort Sea SIC was 2.3E-05. All verification metrics were within the acceptable criteria. The model successfully predicted all instances of below normal (BN) SIC years which are reflected by the FAR (BN) value of 0 and a POD (BN) value of 1.
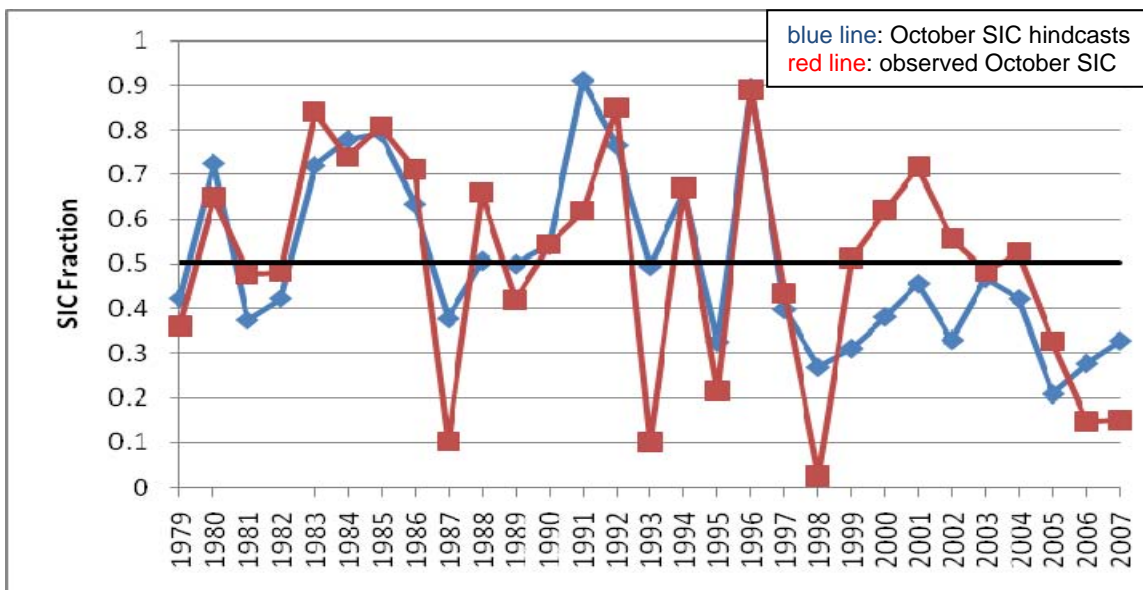
Figure 28. Time series of observed (red) and one-month lead hindcasted (blue) October SIC in the Beaufort Sea for 1979–2007. Hindcasts are based on linear regression using predictor set 1 values from the preceding September. See Table 12 for predictor set 1 variables. The R^2 value was 0.604912. The p-value for Caribbean SSTs was 0.021473, and the p-value for the Beaufort Sea SIC was 2.3E-05. The bold black line indicates the 1979–2007 LTM October SIC in our Beaufort Sea predictand region of 0.5047.

Table 17. Contingency table and verification results for one-month lead hindcasts of October SIC in the Beaufort Sea for 1979–2007. Hindcasts are based on linear regression using predictor set 1 variables. See Chapter II, Section C, 5, for explanations of the contingency table and the verification metrics shown in this table.

Verification of predictor set 1 one-month lead time			
		OBSERVED	
		AN	BN
HINDCASTS	AN	9	0
	BN	4	16
MAE		0.13	
RMSE		0.16	
PC		0.86	
FAR (AN)		0	
FAR (BN)		0.2	
POD (AN)		0.69	
POD (BN)		1	
HSS		0.71	

The predictor set 1 hindcasts at leads of five months to one month were able to predict the general trends and variations of observed SIC in the Beaufort Sea very well. As the lead times got smaller, the R^2 values increased and the predictor p-values remained small and acceptable. This indicates that Caribbean SSTs and Beaufort Sea SIC in previous months are viable predictors of October SIC in the Beaufort Sea at all lead times.

2.   Predictor Set 2

The predictor set 2 variables were Caribbean SSTs, SIC in the Beaufort Sea, and 5 m ocean temperatures in the Beaufort Sea (Table 12). The predictor set 1 hindcasts showed that Caribbean SSTs and Beaufort Sea SIC were viable

predictors. The hindcasts generated using predictor set 2 allowed us to determine whether adding another predictor to the regression model would improve the model performance.

Figure 29 shows the results of the two month lead hindcasts of October 1979–2007 SIC using predictor set 2. The R^2 value was 0.56198, slightly smaller than when using predictor set 1 (Figure 27). The p-values were acceptable (0.12738 for Caribbean SSTs and 0.0005 for Beaufort Sea SIC), except for the 5 m ocean temperatures for which the p-value was 0.94243. Therefore, we did not reject the null hypothesis that in the presence of the other predictors, 5 m ocean temperatures do not influence October SIC. We looked at the relationship between August Beaufort Sea SIC and August Beaufort Sea 5 m ocean temperatures and found that there was a significant relationship between the two variables, with a correlation coefficient of -0.5651 (i.e., low (high) SIC tends to correspond to high (low) ocean T). Ocean temperatures in the Beaufort Sea in previous months have a significant relationship with October SIC, which is evident in Table 11. But ocean temperatures also have a significant correlation with concurrent SIC, indicating multi-colinearity. So including both variables as predictors results in a high p-value for ocean temperature because of its strong relationship with the SIC predictor.   We concluded from this that while ocean temperature in previous months have a strong relationship with SIC in October, ocean temperature can be left out of the regression, as long as previous SIC is included. These results indicate that SIC in previous months can be viewed as a proxy for ocean temperatures (i.e., from a physical perspective, low (high) SIC is associated with high (low) ocean T). Similar results were observed for other lead times (not shown).
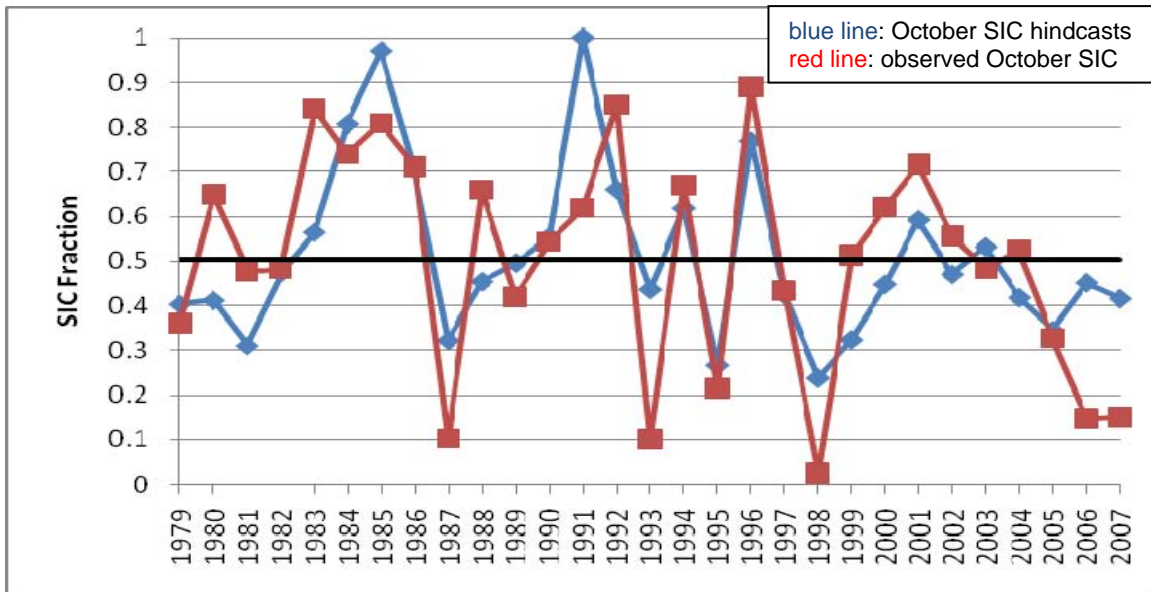
Figure 29.   Time series of observed (red) and two-month lead hindcasted (blue) October SIC in the Beaufort Sea for 1979–2007. Hindcasts are based on linear regression using predictor set 2 values from the preceding August. See Table 12 for predictor set 2 variables. The R^2 value was 0.56198. The p-value for Caribbean SSTs was 0.12738, the p-value for the Beaufort Sea SIC was 0.0005, and the p-value for the 5 m ocean temperatures was 0.94243. The p-value for the 5 m ocean temperatures was too large to be acceptable. The bold black line indicates the 1979–2007 LTM October SIC in our Beaufort Sea predictand region of 0.5047.

3.   Predictor Set 3

Predictor set 3 contained Caribbean SSTs, SIC in the Beaufort Sea, 5m ocean temperatures in the Beaufort Sea, and Z at 850 hPa north of the Beaufort Sea (Table 12). Figure 30 shows the time series of the hindcasted October 1979-2007 SIC values using predictor set 3 and a two month lead time, along with the actual October 1979-2007 values in the Beaufort Sea. The R^2 value was 0.55831, the p-value for Caribbean SSTs was 0.134851, the p-value for the Beaufort Sea SIC was 0.001346, the p-value for the 5m ocean temperatures was 0.94243, and the p-value for the Beaufort Sea 850 hPa Z was 0.381132. As we expected, the p-value for 5 m ocean temperatures was too large to be accepted, for the reasons described in the previous section. The p-value for Z at 850 hPa

was also too large to be accepted. Therefore, we did not reject the null hypothesis that 850 hPa Z has no influence on October SIC.

Table 11 shows that the low level geopotential heights over the Beaufort Sea had a significant and consistent relationship with October SIC at a leads of two and three months. We analyzed the relationship between August SIC in the Beaufort Sea and August Z at 850 hPa in the Beaufort Sea and found a significant relationship between the two variables with a correlation coefficient of -0.323. Similar results were found for the corresponding July correlations. Beaufort Sea Z at 850 hPa has a strong relationship with October SIC at leads of two to three months, but it also has a significant correlation with the concurrent Beaufort Sea SIC. Thus, SIC can be viewed as a proxy for the Beaufort Sea Z at 850 hPa. Physically, this indicates that anomalously westerly (easterly) winds over the Beaufort Sea tend to be associated with high (low) SIC in the Beaufort Sea, consistent with the composite analysis results shown in Figures 17–18. Despite its strong relationship with October SIC, Z 850 hPa can be left out of the regression equations, as long as SIC is included as a predictor.
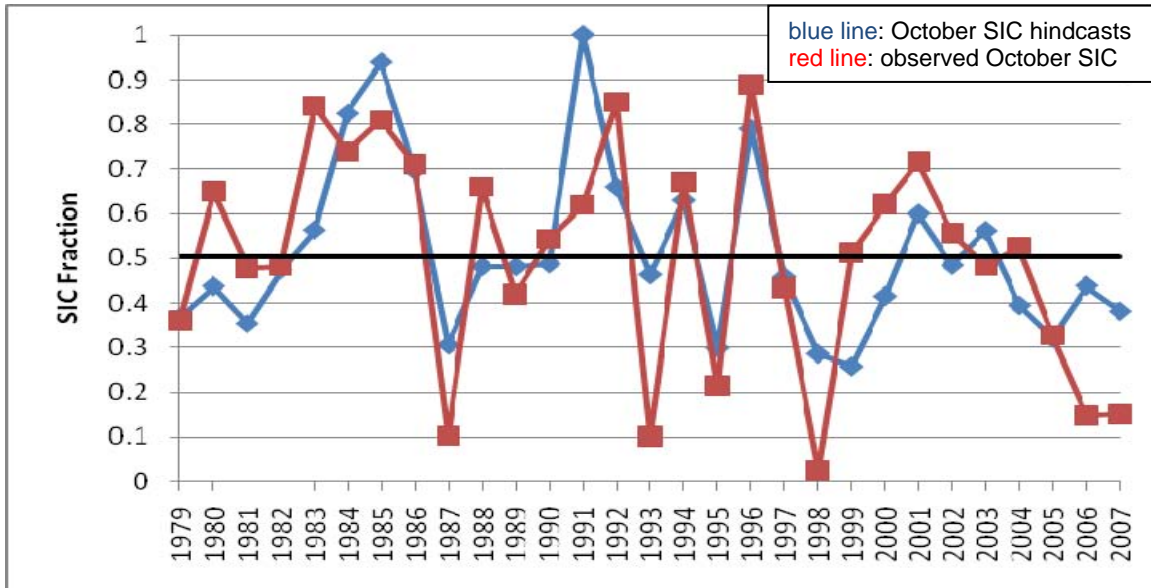
Figure 30.   Time series of observed (red) and two-month lead hindcasted (blue) October SIC in the Beaufort Sea for 1979–2007. Hindcasts are based on linear regression using predictor set 3 values from the preceding August. See Table 12 for predictor set 3 variables. The R^2 value was 0.55831. The p-value for Caribbean SSTs was 0.134851, the p-value for the Beaufort Sea SIC was 0.001346, the p-value for the 5 m ocean temperatures was 0.94243, and the p–value for the Beaufort Sea 850 hPa Z was 0.381132. The p-value for the 5 m ocean temperatures and Z 850 hPa were too large to be acceptable. The bold black line indicates the 1979–2007 LTM October SIC in our Beaufort Sea predictand region of 0.5047.

4.   Predictor Set 4: Special Cases

We investigated several special cases. For brevity, we show only two in this report. First, based on the results summarized in Table 11, we chose three predictors for two month lead hindcasts: (a) August SIC in the Beaufort Sea; (b) air temperature near the Icelandic Low; and (c) Z 850 hPa near the Icelandic Low. The R^2 value was 0.662973, the p-value for Beaufort Sea SIC was 0.001201, the p-value for the surface air temperatures south of Iceland was 0.095677, and the p-value for the Z 850 hPa in the Icelandic Low was 0.088051. Figure 31 shows the results of the hindcasts of October 1979-2007 SIC based on these three predictors as well as the actual October SIC. The R^2 value increased

from 0.578 using the predictor set 1 combination to 0.662973 with the use of this special predictor combination. All three p-values were small and acceptable. The data indicates that the model was able to capture the general trend and variation of SIC well. This indicates that at a two month lead, this special set of predictors will tend to outperform predictor sets 1, 2, and 3.
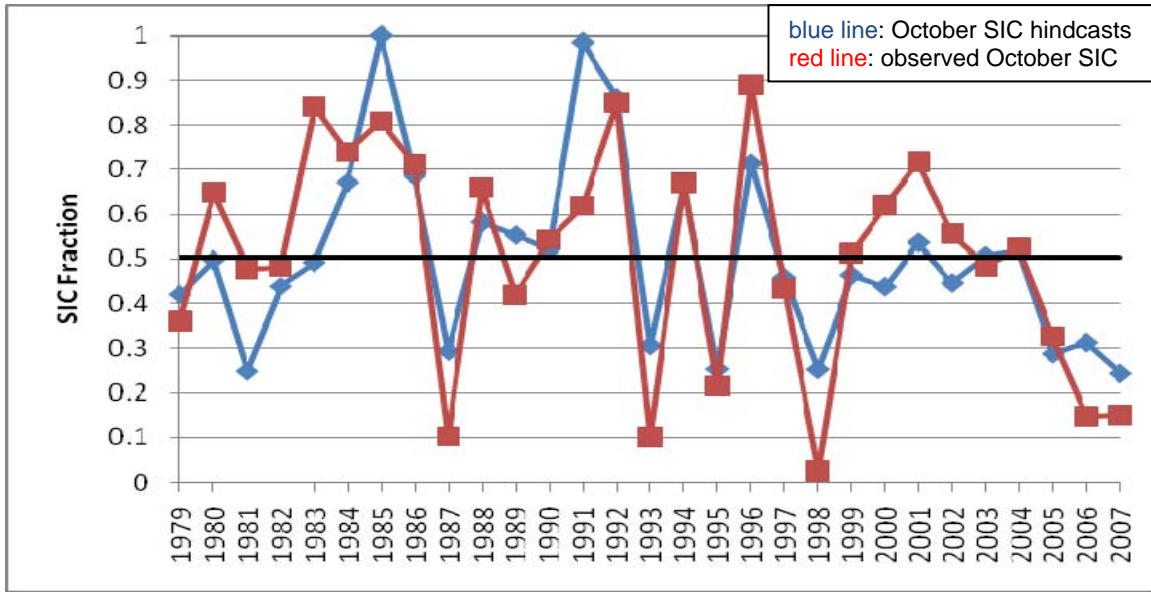
Figure 31. Time series of observed (red) and two-month lead hindcasted (blue) October SIC in the Beaufort Sea for 1979–2007. Hindcasts are based on linear regression using predictor set 4 values from the preceding August, which includes Z 850 hPa in the Icelandic Low, surface air temperatures south of Iceland, and SIC in the Beaufort Sea. The R^2 value was 0.662973. The p-value for Beaufort Sea SIC was 0.001201, the p-value for the surface air temperatures south of Iceland was 0.095677, and the p-value for the Z 850 hPa in the Icelandic Low was 0.088051. The bold black line indicates the 1979–2007 LTM October SIC in our Beaufort Sea predictand region of 0.5047.

The second special case was the use of two predictors—September SIC and surface air temperatures over Alaska— to predict October SIC at a lead of one month. These two predictors were chosen for this lead time based on the results summarized in Table 11. Figure 32 shows the results of the hindcasts of October SIC in the Beaufort Sea using these predictors at a lead of one month, as well as the actual October SIC values. The R^2 value was 0.63893, the p-

value for Beaufort Sea SIC was 0.00248, and the p-value for the surface air temperatures was 0.000591. The data shows that these predictors were able to predict the October SIC for most of the years during 1979-2007 very well. The notable exceptions were 1987, 1993, 2001, and 2007. The R^2 value jumped from approximately 0.60 from the Option 1 predictor combination to approximately 0.64. Both p-values were small and acceptable. This indicates that at a one month lead, this special set of predictors will tend to outperform predictor sets 1.
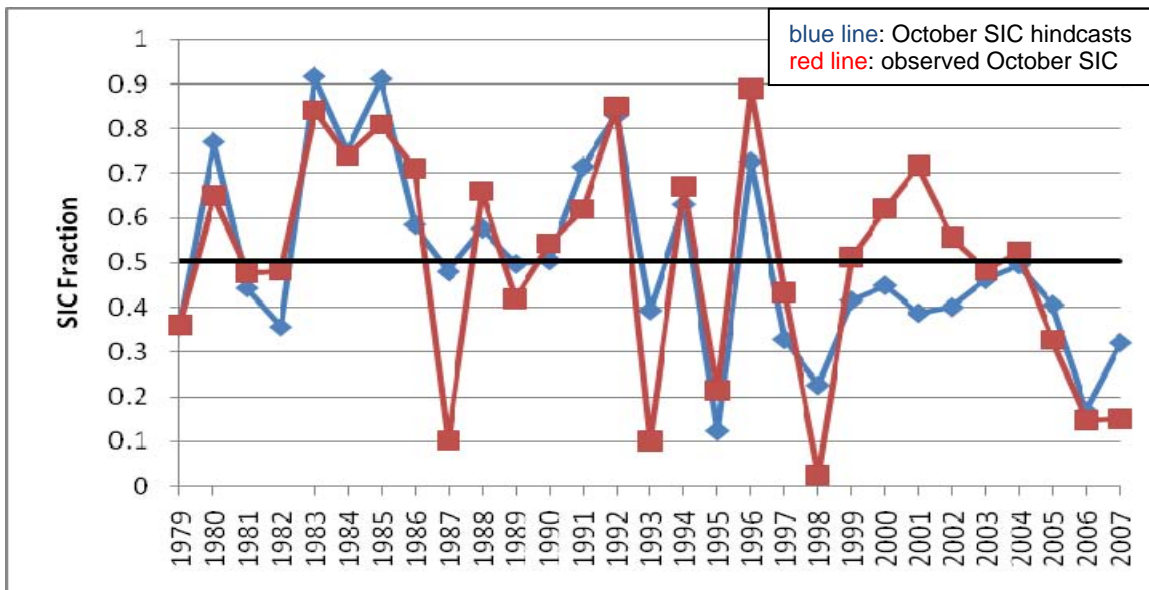

Figure 32.   Time series of observed (red) and one-month lead hindcasted (blue) October SIC in the Beaufort Sea for 1979–2007. Hindcasts are based on linear regression using predictor set 4 values from the preceding September, which includes SIC in the Beaufort Sea and surface air temperatures over Alaska. The R^2 value was 0.63893. The p-value for Beaufort Sea SIC was 0.00248, and the p-value for the surface air temperatures was 0.000591. The bold black line indicates the 1979–2007 LTM October SIC in our Beaufort Sea predictand region of 0.5047.

C.   SUMMARY AND DISCUSSION OF RESULTS

We used composite, correlation, and teleconnection analyses to identify several different sets of predictors to use in producing long range forecasts of SIC in the Beaufort Sea in October (Tables 11–12). We tested these predictor

sets by generating hindcasts based on multivariate linear regression of October SIC in the Beaufort Sea during 1979–2007 at lead times of one to five months. We concluded that, overall, the optimal combination of predictors was antecedent SIC in the Beaufort Sea and SSTs in the Caribbean Sea. Both variables showed a significant and consistent relationship between Beaufort Sea SIC in October at all tested lead times. If Beaufort Sea SIC amounts are above (below) average in earlier months, then Beaufort Sea SIC tends be above (below) average in October too. If Caribbean SSTs are below (above) average in earlier months, then Beaufort Sea SIC tends to be above (below) average in October.

There were other variables that we tested along with Beaufort Sea SIC and Caribbean SSTs that showed a significant relationship with October SIC. Table 11 shows that 5 m ocean temperatures and low level atmospheric circulation in the Beaufort Sea had a noticeable relationship with October SIC at all lead times. We found that while both of these variables show a strong relationship with October SIC, they also showed a significant relationship with Beaufort Sea SIC during simultaneous months. For example, August Beaufort Sea SIC has a significant relationship with August 5 m ocean temperatures with a correlation coefficient of -0.565. August Beaufort Sea SIC also had a correlation coefficient of -0.321 with August Z at 850 hPa. Having these two variables as part of the predictor combination along with antecedent SIC resulted in p-values that indicated that they were not significant predictors in the presence of the antecedent SIC predictor. We concluded that this occurred because of their strong relationship with SIC. As long as SIC is included in the predictor combination, 5 m ocean temperatures and Beaufort Sea circulation can be left out as a predictor. SIC could be viewed as proxy for both 5 m ocean temperature and Z at 850 hPa.

We also tested special cases where predictors were removed and/or replaced with other predictors that showed a significant relationship at specific lead times. We found that at a two month lead time, using August Beaufort Sea SIC, and both August surface air temperatures and Z at 850 hPa in the vicinity of

the Icelandic Low resulted in a higher R^2 than when using the antecedent Beaufort Sea SIC and the Caribbean SST predictor set. At a two month lead time, the Z in the Icelandic Low region showed a stronger relationship with October SIC than Caribbean SSTs, but this did not hold true at the other lead times. We also found that at a one month lead time, the use of September SIC and air temperatures in the Alaska region resulted in a higher R^2 value than when using the September SIC and the Caribbean SST predictor set. At a one month lead time, Alaska surface air temperature showed a stronger relationship with October SIC than did Caribbean SSTs, but this did not hold true at the other lead times.

For operational purposes, the antecedent Beaufort Sea SIC and Caribbean SST predictors may be the most viable predictor set, since it would allow forecasters to use just one basic forecast model for all forecasts at leads of five months to one month.

Our correlation results led us to identify Caribbean SST as a potential predictor, and our hindcast results indicate that it is a useful predictor. However, it is important to determine whether it is also a dynamically plausible predictor. The SIC-SST correlation results in Figure 22 show a North Atlantic pattern similar to the SST anomaly patterns associated with the AO and NAO (Murphree 2008c). This suggests that Caribbean SST may be a proxy for dynamical processes by which the AO and/or NAO affect Beaufort Sea SIC. To test this hypothesis, we investigated the correlations between SST, the AOI, the NAOI, and SIC in the Beaufort Sea.

Figure 33 shows a map of the correlation between the AO index in August-November and north Atlantic SSTs in the following March–June. Note the pronounced quadripole pattern in Figure 33 (negative in tropics-subtropics and subpolar regions, positive in midlatitudes and polar regions) and its resemblance to the north Atlantic patterns, especially the Caribbean patterns, in the maps of the correlations between October SIC and global SSTs (Figure 22). The correlations in Figure 33 indicate that the AO in the late summer and fall

tends to alter the ocean in ways that persist into the following spring. Correlation maps like those in Figure 33, but for correlations with the NAO index (not shown), yield similar patterns, as expected given the close correlation between the AO and NAO (Murphree 2008c).
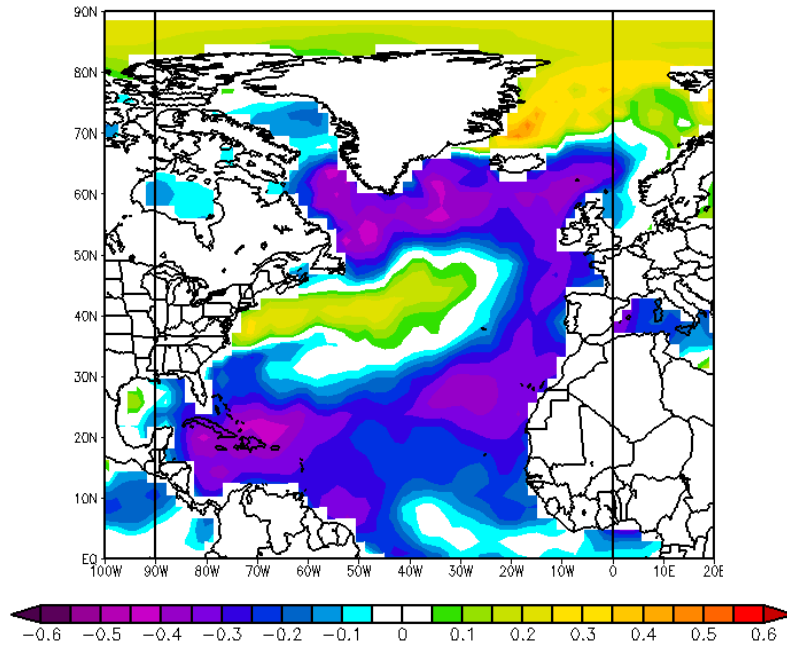
Figure 33. Map of correlations between the AO index in August-November and north Atlantic SSTs in the following March-June. Negative (positive) correlations indicate that when AO index is high, SST tends to be low (high). Correlations with magnitudes ≥ 0.363 are significant at the 95% level (see Chapter II, Section C. 2). Note the quadripole pattern with negative correlations in the tropics and subtropics, positive correlations in much of the midlatitudes, negative correlations in the subpolar region, and positive correlations in the polar region. These correlations indicate that the impacts of late summer and fall AO conditions on north Atlantic SSTs tend to persist into the following spring and summer. Note the strong resemblance between the correlation patterns shown in Figure 22 and Figure 33.

Figure 34 shows time series of the correlation coefficients between Beaufort Sea SIC in the current year October and the AO and NAO indices in the preceding 15 months of the current year and past year. The strongest correlations are in August-November of the past year and May–August of the current year. Tables 6-10 also show correlations between Beaufort Sea SIC in October and the AO and NAO indices in the preceding five to one months. At

these leads, the correlations with SIC are weak compared to those of other potential SC predictors and are statistically insignificant at several leads. In particular, the correlations with the AO and NAO indices are weak compared to those with Caribbean SST (Tables 6-10). However, as indicated by Figures 33–34, the strong Caribbean SST correlations are very likely to be due, at least in part, to the impacts of the AO and/or NAO in the Caribbean during the preceding August-November. If so, then the Caribbean SST predictor may be viewed as a proxy for the delayed effects of the AO and/or NAO in August-November of the past year on Beaufort Sea SIC in October of the current year. These results also indicate that the AO and NAO indices should be considered for use as predictors of Beaufort Sea SIC at leads of 11–15 months (see Chapter IV, Section C).
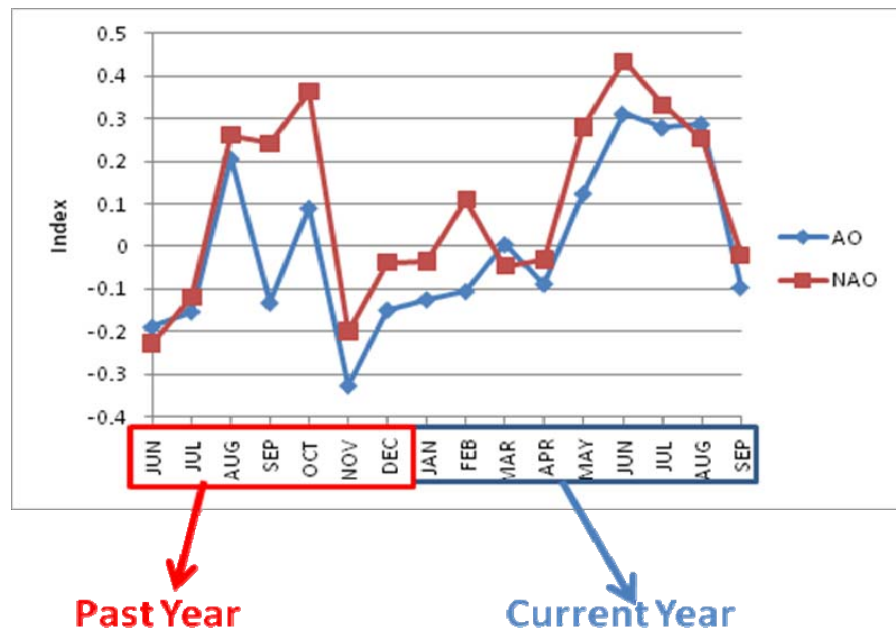
Figure 34. Time series of the correlation coefficients between Beaufort Sea SIC in the current year October and the AO and NAO indices in the preceding 15 months of the current year and past year. A peak exists in the correlation between the AO and NAO indices in the past year August-November and the October SIC in the current year. These correlations, plus those shown in Figure 33, indicate that north Atlantic SSTs in the current year may represent the impacts of the past year AO and NAO conditions on current year SIC conditions in the Beaufort Sea. Thus, north Atlantic SSTs may be useful predictors of the long term impacts of the AO and NAO on Arctic sea ice (e.g., Caribbean Sea SSTs may be useful predictors of Beaufort Sea sea ice).

D.   LONG RANGE FORECAST RESULTS

We conducted an additional test of our forecast methods by issuing a forecast on 01 June 2010 of SIC in the Beaufort Sea in October 2010. To develop this forecast at a five month lead time, we obtained and applied the May 2010 monthly average Caribbean SSTs and the May 2010 monthly average Beaufort Sea SIC. We developed a linear regression model based on using May 1979–2007 Caribbean SSTs and Beaufort Sea SIC as the predictors and October 1979-2007 SIC as the predictand. The regression equation was:

$$Y = 8.3625 + 1.708x_1 - 0.341x_2 \qquad (7)$$

Y is the forecasted October 2010 SIC amount, x_1 is the May 2010 monthly average SIC in the Beaufort Sea, and x_2 is the May 2010 monthly average Caribbean SST. The May 2010 Beaufort Sea SIC was 0.944, slightly above the May LTM SIC of 0.92102. The May 2010 Caribbean SST was 28.2°C, noticeably higher than the May LTM Caribbean SST of approximately 27.7°C. We used these May 2010 predictors values and equation 7 to produce a forecast of Beaufort Sea SIC in October 2010 of 0.33748. The LTM Beaufort SIC in October is 0.5047. Therefore, our forecasted SIC in October 2010 is 37% below the average SIC for October. Figure 35 shows time series of May Beaufort Sea SIC, May Caribbean SSTs, and October SIC. Also shown are the May 2010 values of Beaufort Sea SIC and Caribbean SSTs, and our forecasted SIC for October 2010. We will verify our forecast in November 2010.
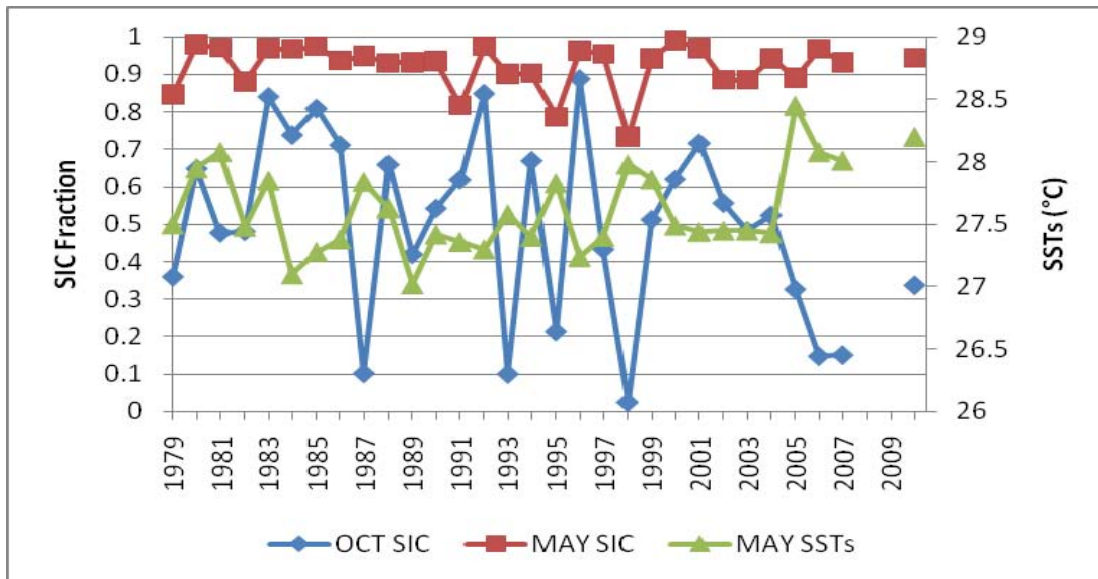
Figure 35.   Time series of October SIC in Beaufort Sea for 1979–2007: observed (blue line) and forecasted at a five-month lead time for October 2010 (single blue diamond on right side of figure). Forecast issued 01 June 2010. Also shown are time series of the predictors in the linear regression model used to produce the SIC hindcasts and forecast: red line = May SIC in the Beaufort Sea; green line = May SST in the Caribbean Sea. The May 2010 observed values of the predictors are shown by the green triangle (SST) and red square (SIC) on the right side of the figure.

IV. CONCLUSIONS

A. KEY RESULTS

This study investigated the viability of using advanced climate data sets and methods to generate skillful probabilistic forecasts at long lead times of Arctic SIC. Our focus was on SIC in the Beaufort Sea in October. One of our primary goals was to contribute to the improvement of operational long-range support products for Navy decision makers planning Arctic.

The methods we used in this study (overviewed in Chapter II) apply existing and easily available state of the science atmospheric, oceanic, and ice data sets. These data sets were used to carry out analyses of the climate variations in Arctic sea ice and the overlying atmosphere and ocean. Evaluating the data allowed us to recognize interannual variations and trends in sea ice and the corresponding atmospheric and oceanic patterns associated with sea ice. We selected the Beaufort Sea as the region to predict SIC based on its high SIC variation, its location within the Northwest Passage, and its overall importance to the U.S. and its allies. We selected October as our target forecast time period based on the potential problems that increasing sea ice poses during this month. We correlated October SIC in the Beaufort Sea with several different atmospheric and oceanic variables and looked at composite anomalies of these variables for years when SIC was high and low in the Beaufort Sea. From this, we found that Beaufort Sea SIC and Caribbean SSTs at lead times of one to five months were a predictor combination that was consistently and significantly correlated with October SIC in the Beaufort Sea. We generated hindcasts of 1979–2007 October SIC by means of a multivariate linear regression model based on these two predictors. We measured the skill of the hindcasts by using scalar and tercile metrics (outlined in Chapter II) and concluded that Beaufort Sea SIC and Caribbean SSTs during previous months are viable predictors of

October SIC in the Beaufort Sea. Based on observed Beaufort Sea SIC and Caribbean SSTs in May 2010, we developed and issued in June 2010 a long lead climate forecast of Beaufort Sea SIC.

In additional testing, we found that 5 m ocean temperatures and low level atmospheric circulation over the Beaufort Sea during previous months show a signification relationship with Beaufort Sea SIC in October, but that both variables may be left out of the regression as long as the corresponding month's Beaufort SIC amount is included in the regression. This is because of the strong relationship that both 5 m ocean temperatures and the atmospheric circulation have with the concurrent Beaufort SIC. Therefore, Beaufort Sea SIC can be viewed as a proxy for both variables. As long as Beaufort Sea SIC is included in the regression, the other two variables can be left out.

We also found that at a two month lead time, Caribbean SSTs can be replaced with surface air temperatures and low level atmospheric circulation (Z at 850 hPa) near the Icelandic Low circulation, with a higher R^2 being obtained than when using Caribbean SSTs. At a one month lead time, Caribbean SSTs can be replaced with average surface air temperatures in the Alaska/Beaufort Sea region to obtain a higher R^2 value. This could indicate that the August Icelandic Low conditions and September Beaufort Sea conditions have a stronger relationship with October SIC than Caribbean SSTs. While these are intriguing findings, using Caribbean SSTs might still be preferred at these lead times for consistency in forecasting operations, the values forecasted at different leads, and the use of the forecasts by decision makers.

There is evidence that the AO and/or NAO from the previous summer-fall can influence in the following spring the upper ocean in the north Atlantic including the Caribbean Sea. Alterations in the Caribbean SSTs can lead to altered climate patterns resulting in variations in SIC in the Beaufort Sea in October. The dynamical and physical processes that occur in this changed climate system and their connection to Beaufort Sea SIC need to be researched further.

Our results indicate that viable long-range forecasts of October SIC in the Beaufort Sea are possible via the use of Beaufort Sea SIC and Caribbean SSTs at lead times of one to five months. While our results show a definite correlation between these two variables and October SIC in the Beaufort Sea, we suspect that there are additional factors and dynamics that play an important role in the variability of SIC in the Beaufort Sea. Our study is meant to emphasize how advanced data sets and methods can be used to generate skillful long-range forecasts of sea ice amounts in the Arctic for use in operational planning by the U.S. Navy.

B.   APPLICABILITY TO DOD OPERATIONS

The U.S. Navy Arctic Roadmap (outlined in Chapter I) gives an overview of the Navy's goals concerning present and future operations in the Arctic. The Roadmap outlines several focus areas, but climate assessment and prediction focus area is the basis for success in the other focus areas. The impacts from improving climate assessment and prediction that are outlined in the Roadmap include having a better understanding of when significant access for Arctic navigation is likely to develop, having a better understanding of changes that have occurred in the Arctic environment and what climate changes could occur in the future, and providing Navy decision makers with a better understanding of the Arctic environment on temporal and spatial scales that support naval tactical, operational, and strategic planning.

Arctic climate change has been a heavily research area for the past 10-20 years. Many prior studies have investigated Arctic sea ice variation, although relatively few have investigated long range forecasting of sea ice. There are several organizations (DoD and non-DoD) that offer Arctic seasonal outlooks and short range sea ice forecasts. A 30-day sea ice forecast is generated by the NIC and CIS in the form of a text document. The Navy is currently able to develop a LTM analysis of SIC tailored to a customer's time period and area of interest. The LTM does not account for the interannual variation in sea ice that occurs. This study has contributed to the development of long-range products by the

application of advanced data sets and methods to develop and test new methods for providing Navy decision makers with specific sea ice information tailored to their area and time period of interest. The study, along with Mundhenk (2009), Heidt (2009), Ramsaur (2009), Raynak (2009), Turek (2008), Moss (2007), and Twigg (2007), highlight the importance of using advanced climate data sets and methods to improve our understanding of climate system dynamics, the impacts of climate variations and climate change on DoD operations, and methods for operationally predicting those impacts at long lead times (weeks, months, years, decades, and longer).

C.   TOPICS FOR FURTHER RESEARCH

This and prior studies have demonstrated that the application of advanced climate data sets and methods can improve long lead climate support for operational planning in the Arctic and other regions. But additional research is needed to continue this development. Are recommendations for further research are listed below.

1. This study used a SIC data set that ended in December 2007. To improve the analysis of SIC and its potential predictors, we recommend obtaining SIC data that extends to the present. This may be available from NSIDC. Sea ice data sets from the Hadley Centre should also be investigated.

2. This study used SIC as the only variable to provide information about sea ice variation within the Arctic. There are other sea ice data sets available that could provide a better understanding of sea ice variation (e.g., data on ice thickness and volume, multi-year sea ice, and first year sea ice from NSIDC and other organizations).

3. This study focused on analyzing October SIC in the Beaufort Sea at leads of one to five months. Studies of other predictand regions and periods, and other lead times, are needed to increase our understanding of the potential for forecasting sea ice conditions at long lead times.

4. We found evidence of long term warming trends in the upper ocean of the Arctic when analyzing oceanic reanalysis data. This topic should be

investigated further to help assess and forecast the impacts of upper ocean temperature and temperature advection on Arctic sea ice, ocean acoustic parameters, and other variables.

5. The use of alternate base periods in climate anomaly analyses should be investigated to better account for long term trends.

6. Our study indicated some potential for skillful forecast at leads of a year or more, using as predictors, for example, the AO and NAO indices. Future studies should investigate this potential further.

7. Additional long range forecast methods should be investigated, such as optimal climate normal methods for forecasting variables that are undergoing large low frequency variations (e.g., sea ice in regions experiencing long term declines).

8. Future studies should investigate additional verification methods (e.g., tercile categorical verification).

9. Investigations are needed on the long range forecasting needs of U.S. Navy planners and other decision makers (e.g., information on environmental variables for which forecasts are needed [including quantities other than SIC], operational sea ice thresholds, planning cycles). In order to best meet these customers' needs, more information is needed about the type of analyses and forecasts, and accompanying information (e.g., uncertainty assessments) that are needed for specific operations.

THIS PAGE INTENTIONALLY LEFT BLANK

LIST OF REFERENCES

Arctic Research Consortium of the U.S. (ARCUS) cited 2010; [Accessed online at http://www.arcus.org/.] Accessed May 2010.

Barnett, D. G., 1980: A practical method of long-range ice forecasting for the north coast of Alaska. *Tech. Rep. TR-1 to the Fleet Weather Center*, Suitland, MD, 16 pp.

Carton, J. A., G. Chepurin, X. Cao, and B. Giese, 2000: A Simple Ocean Data Assimilation analysis of the global upper ocean 1950–95. Part I: Methodology. *Journal of Physical Oceanography*, **30**, 294–309.

Carton, J. A., and B. Giese, 2008: A reanalysis of ocean climate using Simple Ocean Data Assimilation. *Mon. Weather Rev.*, **136**, 2999–3017.

Comiso, J. C., C. L. Parkinson, R. Gersten, and L. Stock, 2008, Accelerated decline in the Arctic sea ice cover, *Geophys. Res. Lett.,* **35**, L01703, doi:10.1029/2007GL031972.

Deser, C. and H. Teng, 2008, Evolution of Arctic sea ice concentration trends and the role of atmospheric circulation forcing, 1979-2007, *Geophys. Res. Lett.,* **35**, L02504, doi:10.1029/2007GL032023.

Drobot, S., 2003: Long-range forecasting of ice severity in the Beaufort-Chukchi Sea. *Weather and Forecasting*, Vol. 18, pp 1161–1175.

Earth Systems Research Laboratory (ESRL), cited 2010. [Accessed online at http://www.cdc.noaa.gov/cgi-bin/PublicData/getpage.pl.] Accessed May 2010.

Heidt, S., 2009: Long-Range Atmosphere-Ocean Forecasting in Support of Undersea Warfare Operations in the Western North Pacific. M.S. thesis, Dept. of Meteorology, Naval Postgraduate School, pp 99.

Kalnay, E., and Coauthors, 1996: The NCEP/NCAR 40-year reanalysis project. *Bull. Amer. Meteor. Soc*, **77**, 437–471.

Kistler, R., and Coauthors, 2001: The NCEP-NCAR 50-Year Reanalysis: Monthly Means CD-ROM and Documentation. Bull. Amer. Meteor. Soc., **82**, 247–268.

Lindsay, R. W., J. Zhang, A. J. Schweiger, M. A. Steele, 2007: Seasonal predictions of ice extent in the Arctic Ocean. *Journal of Geophysical Research*, Vol. 113, C02023, doi: 10.1029/2007JC004259.

Lindsay, R., J. Zhang cited 2010: Predictions of Alaskan summer ice conditions from May 2010 [Accessed online at http://www.arcus.org/files/search/sea-ice-outlook/2010/06/pdf/regional/lindsayzhangjuneoutlook.pdf.] Accessed June 2010.

Liu, J., J. A. Curry, and Y. Hu, 2004, Recent Arctic sea ice variability: connections to the Arctic Oscillations and the ENSO, *Geophys. Res. Lett.*, **31**, L09211, doi:10.1029/2004GL019858.

Maslowski, W., J. C. Kinney, J. Jakacki, 2007: Toward prediction of environmental Arctic change. *Computing in Science and Engineering*, November/December 2007, pp. 2–7.

Moss, S. M., 2007: Long-Range Operational Military Forecasts for Afghanistan. M.S. thesis, Dept. of Meteorology, Naval Postgraduate School, 99 pp.

Mundhenk, B. D., 2009: A Statistical-Dynamical Approach to Intreaseasonal Prediction of Tropical Cyclogenesis in the Western North Pacific. M.S. thesis, Dept. of Meteorology, Naval Postgraduate School, 107 pp.

Murphree, T., 2008a: *MR3610 Course Module 6: Smart Climatology*. Dept. of Meteorology, Naval Postgraduate School, Monterey, California.

Murphree, T., 2008b: *MR3610 Course Module 11: Ocean Role in Climate System Part 2*. Dept of Meteorology, Naval Postgraduate School, Monterey, California.

Murphree, T., 2008c: *MR3610 Course Module 22: North Atlantic Oscillation and Arctic Oscillation.* Dept of Meteorology, Naval Postgraduate School, Monterey, California.

National Ice Center (NIC) cited 2010: NAIS Seasonal Outlooks and 30-Day Forecasts [Accessed online at http://www.natice.noaa.gov/products/nais_forecasts.html.] Accessed May 2010.

National Snow and Ice Data Center (NSIDC) cited 2010a: Arctic Sea Ice News and Analysis [Accessed online at http://nsidc.org/arcticseaicenews/index.html.] Accessed May 2010.

National Snow and Ice Data Center (NSIDC) cited 2010b: Sea Ice Concentrations from Nimbus -7 SMMR and DMSP SSM/I Passive Microwave Data [Accessed online at http://nsidc.org/data/docs/daac/nsidc0051_gsfc_seaice.gd.html.] Accessed May 2010.

National Snow and Ice Data Center (NSIDC) cited 2010c: Questions about Arctic sea ice [Accessed online at http://nsidc.org/arcticseaicenews/faq.html#area_extent.] Accessed May 2010.

North American Ice Service (NAIS) citied 2010. [Accessed online at http://nais-sgan.org/.] Accessed May 2010.

Ramsaur, D. C., 2009: Climate Analysis and Long-Range Forecasting of Radar Performance in the Western North Pacific. M.S. thesis, Dept. of Meteorology, Naval Postgraduate School, 115 pp.

Raynak, C., 2009: Statistical-Dynamical Forecasting of Tropical Cyclogenesis in the North Atlantic at Intraseasonal Lead Times. M.S. thesis, Dept. of Meteorology, Naval Postgraduate School, 93 pp.

Reynolds, R., and Coauthors, 2002: An improved in situ and satellite SST analysis for climate. J. Climate, **15**, 1609-1625.

Saha, S., and Coauthors, 2010: The NCEP Climate Forecast System Reanalysis. Bull. Amer. Meteor. Soc., accepted.

Study of Environmental Arctic Change (SEARCH) cited 2010: Sea Ice Outlook [Accessed online at http://www.arcus.org/SEARCH/seaiceoutlook/index.php.] Accessed May 2010.

TFCC 2009: U.S. Navy Arctic Roadmap, Task Force Climate Change / Oceanographer of the Navy, October 2009, 33 pp.

Titley, RADM D., 2009: *The U.S. Navy's Arctic Roadmap.* EUCOM High North Conference.

Tomczak, M., J. S. Godfrey, 1994: *Regional Oceanography: An Introduction*, Pergamon, 422 pp.

Tseng, Hsien-Liang R., 2010: Toward Quantifying the Impact of Atmospheric Forcing on Arctic Sea Ice Variability using the NPS 1/12 Degree Pan-Arctic Couples Ice-Ocean Model. M.S. thesis, Dept. of Meteorology, Naval Postgraduate School, Monterey, California, 169 pp.

Turek, A., 2008: Smart Climatology Applications for Undersea Warfare. M.S. thesis, Dept. of Meteorology, Naval Postgraduate School, Monterey, California,

Twigg, K.L., 2007: A Smart Climatology of Evaporation Duct Height and Surface Radar Propagation in the Indian Ocean. M.S. thesis, Dept. of Meteorology, Naval Postgraduate School, Monterey, California, 135 pp.

van den Dool, H., 2007: *Empirical Methods in Short-Term Climate Prediction*. Oxford University Press, 215 pp.

Wilks, D., 2006: *Statistical Methods in the Atmospheric Science*, Academic Press, 627 pp.

Zhang, J., M. Steele, R. Lindsay, A. Schweiger, and J. Morison, 2008: Ensemble 1-Year predictions of Arctic sea ice for the spring and summer of 2008, Geophys. Res. Lett., 35, L08502, doi:10.1029/2008GL033244.

Zhang, J. cited 2010: Outlook of 9/2010 Arctic sea ice from 6/1/2010 [Accessed online at http://www.arcus.org/files/search/sea-ice-outlook/2010/06/pdf/regional/zhangjuneoutlook.pdf.] Accessed June 2010.

INITIAL DISTRIBUTION LIST

1. Defense Technical Information Center
    Ft. Belvoir, Virginia

2. Dudley Knox Library
    Naval Postgraduate School
    Monterey, California

3. Dr. Tom Murphree
    Naval Postgraduate School
    Monterey, California

4. David Meyer
    Naval Postgraduate School
    Monterey, California